Chapter-4

Synoptic Systems

In the previous chapters, the salient aspects of climatological features of atmospheric circulation and onset process have been discussed. With the onset of NE monsoon, the east-west seasonal trough (ITCZ) slowly shifts southwards. During the season, the mean position of the east-west trough extends from the south Arabian sea to south Bay of Bengal across the south Peninsula. This seasonal trough, an area of large scale convergence, can help formation of low level circulations and low pressure systems, which lead to large scale convection and rainfall over the region.

The main synoptic systems affecting rainfall over the south Peninsula are a) Low pressure areas b) Depressions, cyclonic storms and above c) troughs in easterlies or easterly waves and d) upper air troughs or cyclonic circulations, confined to lower levels. The troughs in easterlies could be observed at sea level or in lower atmosphere. The upper air trough could be generally oriented in an east-west direction.

A summary of different synoptic systems affecting the south peninsula during the NE monsoon season during the period 2000-2019 is given in Table 4.1. These details were obtained from the post-monsoon seasonal reports published by the IMD in ***Mausam***.

Table 4.1

Number of Synoptic systems affecting South Peninsula during the NE monsoon season (Oct-Dec)

Year	Low Pressure areas	Depressions and above	Upper air trough/cyclonic circulation	Trough in Easterlies/ Easterly Wave
2000	2	4	20	3
2001	4	3	8	8
2002	1	4	2	14

2003	4	4	7	11
2004	4	4	3	17
2005	7	5	4	2
2006	2	1	10	18
2007	3	3	20	6
2008	2	5	12	9
2009	3	2	10	10
2010	3	5	10	5
2011	0	5	9	9
2012	2	4	8	13
2013	1	6	8	7
2014	1	2	8	13
2015	6	4	14	7
2016	0	5	12	11
2017	3	5	29	3
2018	2	4	37	8
2019	2	6	22	5
2020	3	3	19	4
2021	4	2	28	7
Mean	2.7	3.9	13.6	8.6
Standard Deviation	1.7	1.3	9.1	4.4

In this table, low pressure areas, depressions and cyclonic storms forming over the south Arabian Sea and South Bay of Bengal are considered. The upper air troughs and cyclonic circulations are counted only those forming near the South peninsula contributing rainfall activity over the region.

On an average, around 3 low pressure systems form during the NE monsoon season, which do not intensify into depressions or above. During the season, four depressions/cyclonic storms can be expected to affect the south peninsula. On an average, 13 upper air cyclonic circulations/troughs and 10 troughs in easterlies/easterly waves also form affecting the south peninsula during the season. While there is little year to year variation in cyclonic storms (Depressions and above), there is, however, large year to year variation in the frequency of tropical easterly waves and upper air systems. It may be interesting to understand the contribution of each of these weather systems on the seasonal rainfall distribution over the region.

A preliminary analysis was made to understand the variability of the frequency of these synoptic systems and its linkage to global forcings like El Nino-Southern Oscillation (ENSO), Pacific Decadal Oscillation (PDO), North Atlantic Oscillation (NAO), Indian Ocean Dipole (IOD) etc. The time series of the global indices were taken from the website https://psl.noaa.gov/gcos_wgsp/Timeseries. The data of the period 2000-2021 (22 years) have been used to calculate the correlation coefficients and the results are given in Table 4.2. The seasonal mean of Oct-Dec period was considered for the analysis.

Table 4.2

Correlations between Global Circulation Indices and frequency of Synoptic systems

Global Index	Lows	Dep/CS	Troughs / Circulations	Easterly Waves
Nino 3.4	0.134	-0.216	-0.180	**0.489**
SOI	-0.109	0.249	0.290	**-0.504**
NAO	-0.084	-0.079	0.172	0.030
AO	-0.036	0.165	0.125	0.008
AMO	-0.036	0.165	0.125	0.008
PDO	-0.181	-0.013	-0.146	0.336
IOD	-0.183	-0.041	**0.386**	0.170

Note: Nino3.4: ENSO Index, SOI: Southern Oscillation Index, NAO: North Atlantic Oscillation. AO: Arctic Oscillation, AMO: Atlantic Multi-decadal Oscillation, PDO: Pacific Decadal Oscillation, IOD: Indian Ocean Dipole.

It is interesting to note that the frequency of easterly waves over the Bay of Bengal during the NE monsoon season has a statistically significant correlation with Nino 3.4 and SOI. This indicates, during the El Nino years, frequency of easterly waves is enhanced, which might lead to more seasonal rainfall over the south peninsula. The relationship between the ENSO and seasonal rainfall is discussed in detail later in the chapter on the NE monsoon variability. The seasonal rainfall is positively correlated with the Nino 3.4 index. It is also interesting to note that Pacific Decadal Oscillation (PDO) plays a positive role in enhancing the frequency of easterly waves. The positive phase of the Indian Ocean Dipole (IOD) leads to more troughs and upper air circulations over south peninsula which also contribute to the seasonal rainfall.

A brief description of various synoptic systems forming during the NE monsoon season is given below with an example, just for illustration. It may be noted that the characteristics of these synoptic systems may show large variability.

4.1. **Trough of low over the Southwest Bay of Bengal (30 Oct - 05 Nov 2018)**

An example of a trough of low pressure that formed over the Southwest Bay of Bengal is discussed below.

A low-level cyclonic circulation was prevailing over the southwest BOB and adjoining Sri Lanka during 27-31 Oct and trough of low at mean sea level extending from this circulation from southwest - west central BOB off TN / south CAP / Sri Lanka coast during 30 Oct - 05 Nov. Fig. 4.1. shows the different aspects of the trough of low which formed over the Southwest Bay, including satellite images and rainfall associated with the system. The average rainfall is taken from the IMD/NCMRWF merged satellite (GPM)-raingauge dataset. The streamline pattern and mean sea level pressure chart are taken from the archives of IMD. These plot shows a north-south trough over the

southwest Bay of Bengal and adjoining Tamil Nadu coast. This trough is observed on the sea level also. The presence of this trough had caused extensive rainfall off the coasts of Tamil Nadu and Sri Lanka (Fig. 4.1 c).

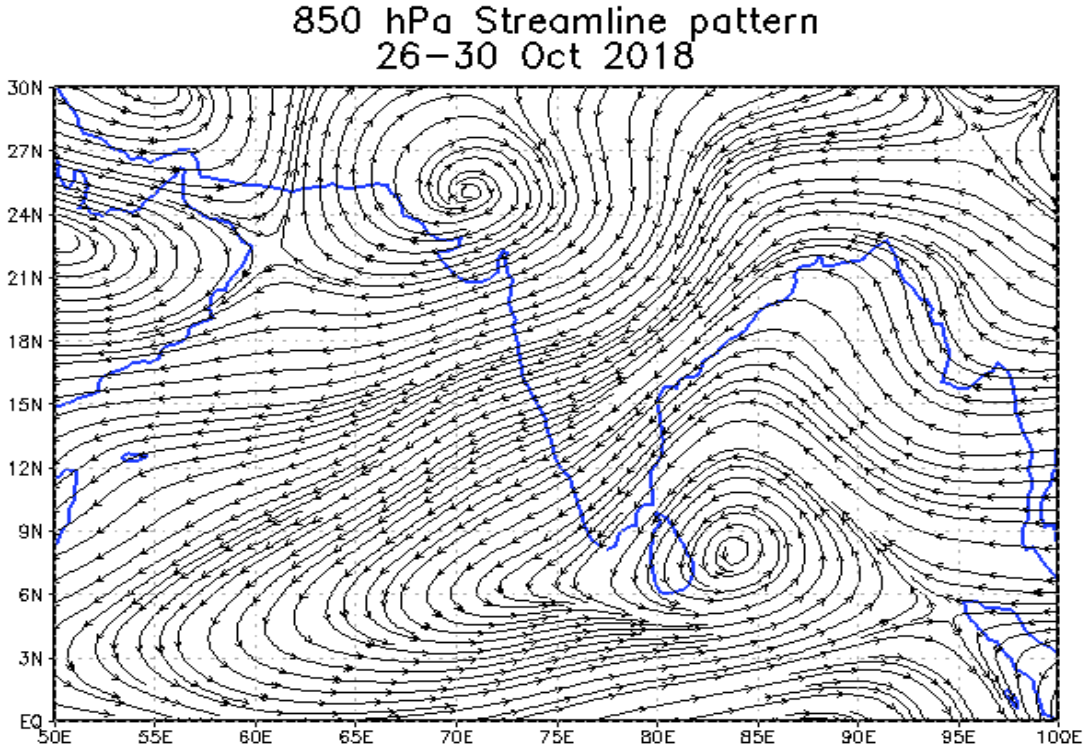

(a)

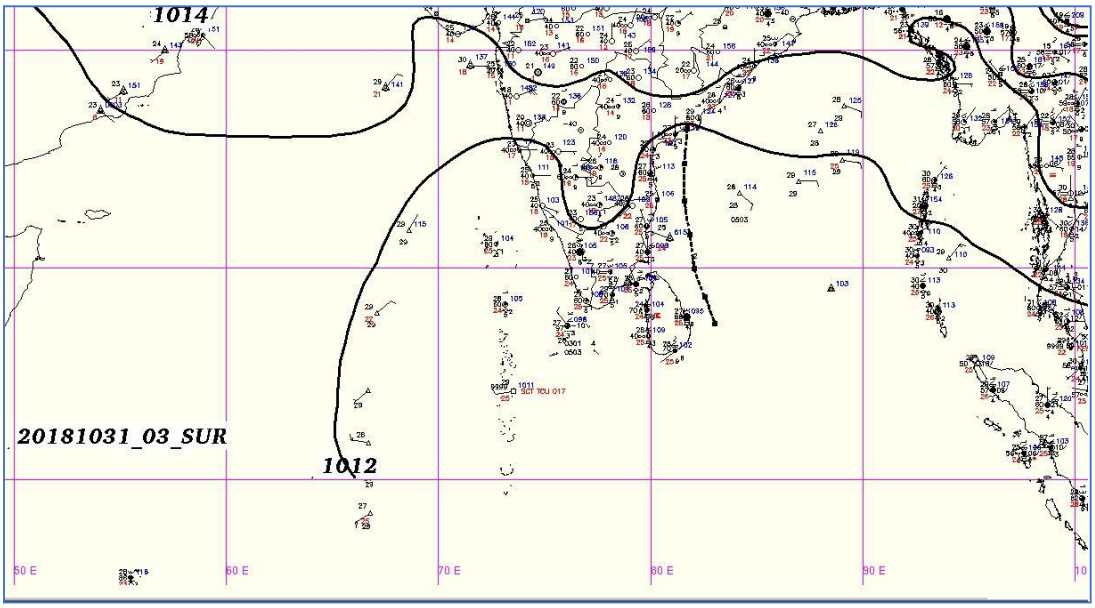

(b)

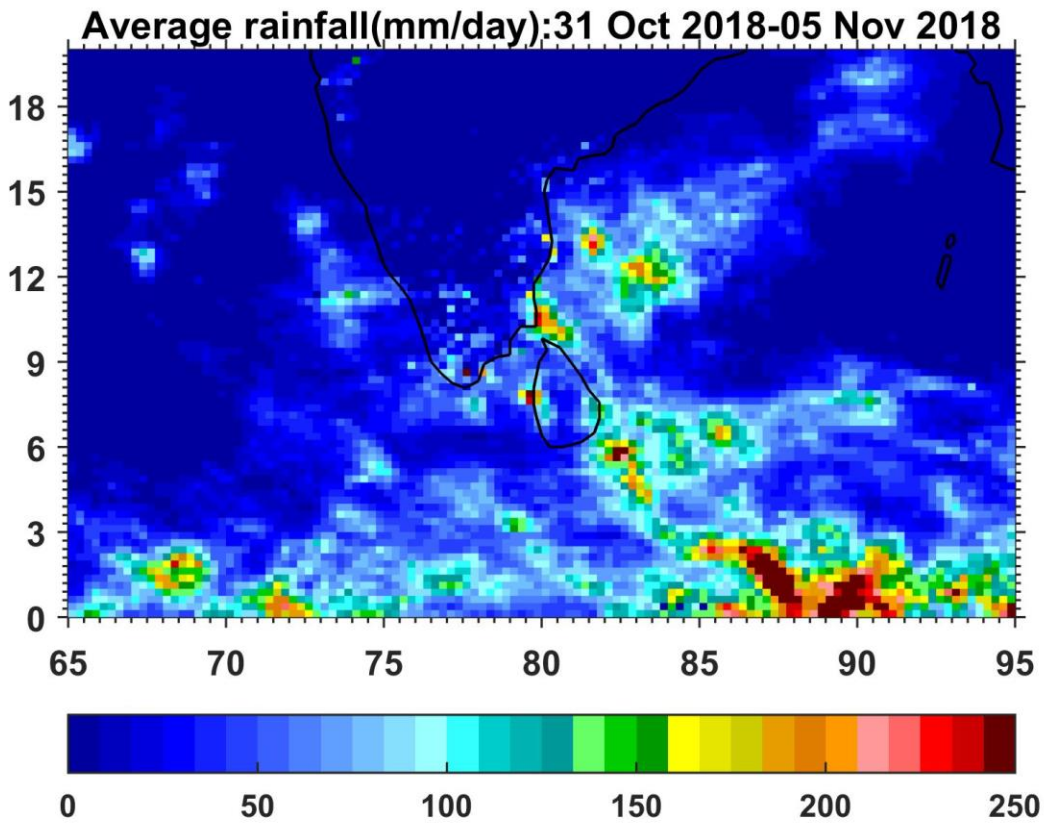

(C)

Fig. 4.1. a) 850 hPa streamline analysis during 26-30 Oct, 2018 b) Isobaric analysis on 31 Oct, 2018 and c) average rainfall (mm/day) during 31 Oct to 05 Nov, 2018.

4.2. **Upper air east-west trough**

During the NE Monsoon season, occurrence of an east-west trough across the south peninsula is very common. This could be associated with the presence of ITCZ over the region. One good example of the east-west trough is shown in Fig. 4.2 a-c. During 14-16 Nov 2021, an east-west trough was present passing across the south peninsula. The east-west trough provides large scale convergence and associated rainfall activity over the region, as seen in the vertical velocity (omega) shown in Fig. 4.2 b. Associated with this east-west trough large scale rainfall activity was observed over the south Peninsula and the Arabian sea.

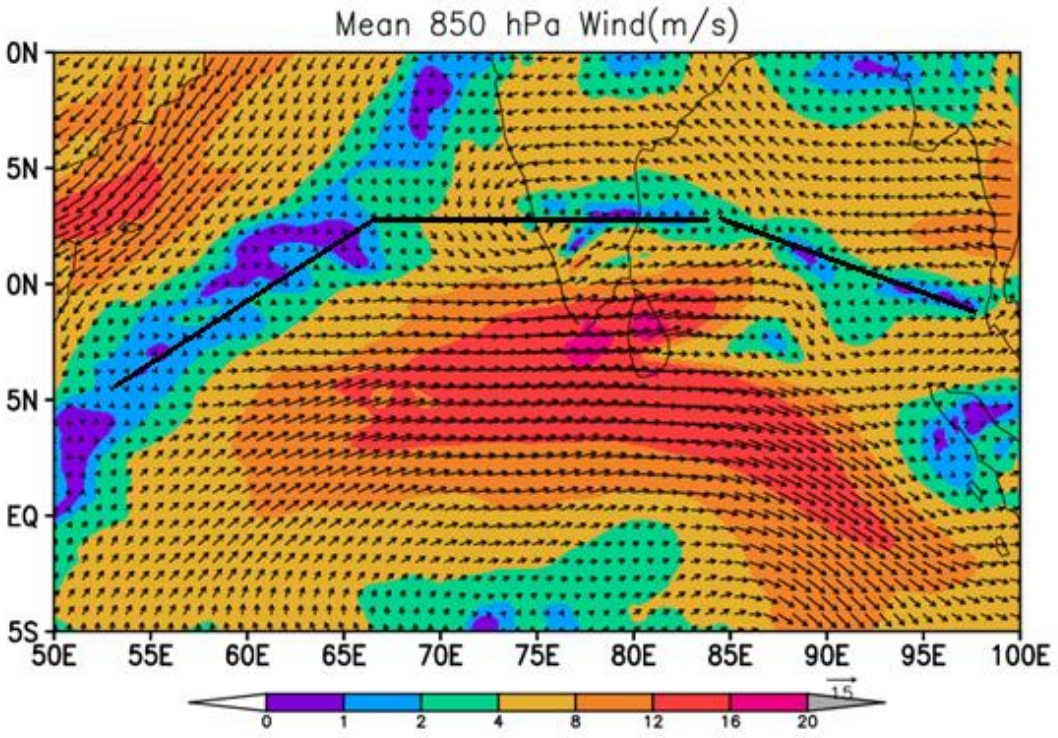
Mean 850 hPa Wind(m/s)
0N
5N
0N
5N
EQ
5S
50E
55E
60E
65E
70E
75E
80E
85E
90E
95E
100E
15
0
1
2
4
8
12
16
20

(a)

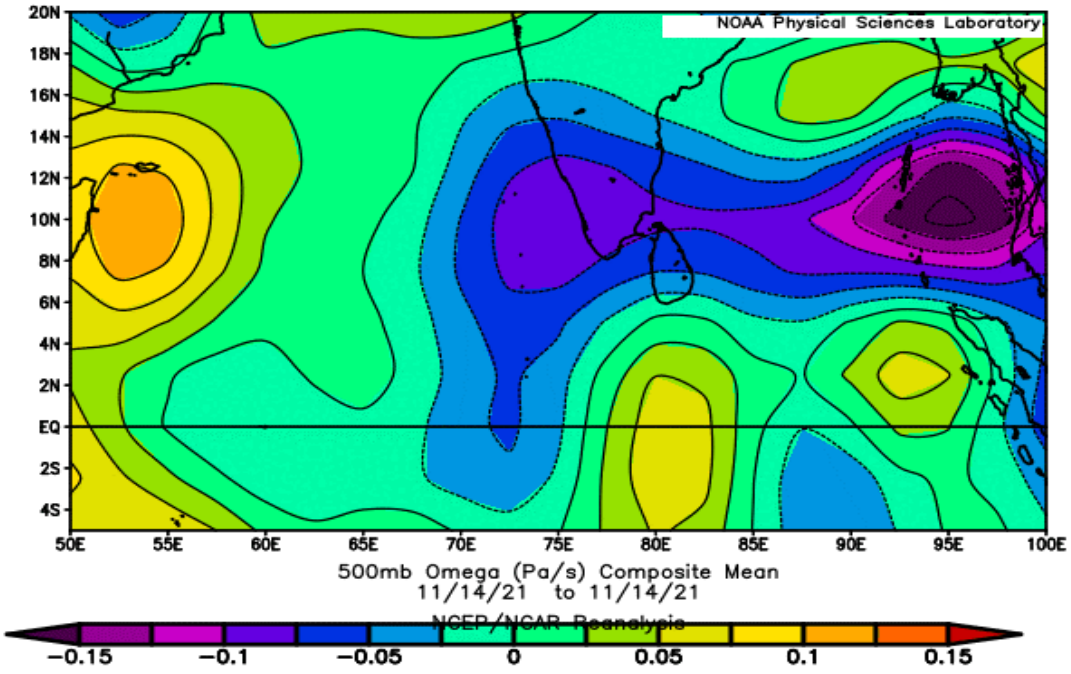
NOAA Physical Sciences Laboratory
20N
18N
16N
14N
12N
10N
8N
6N
4N
2N
EQ
2S
4S
50E
55E
60E
65E
70E
75E
80E
85E
90E
95E
100E
500mb Omega (Pa/s) Composite Mean
11/14/21 to 11/14/21
NCEP/NCAR Reanalysis
−0.15
−0.1
−0.05
0
0.05
0.1
0.15

(b)

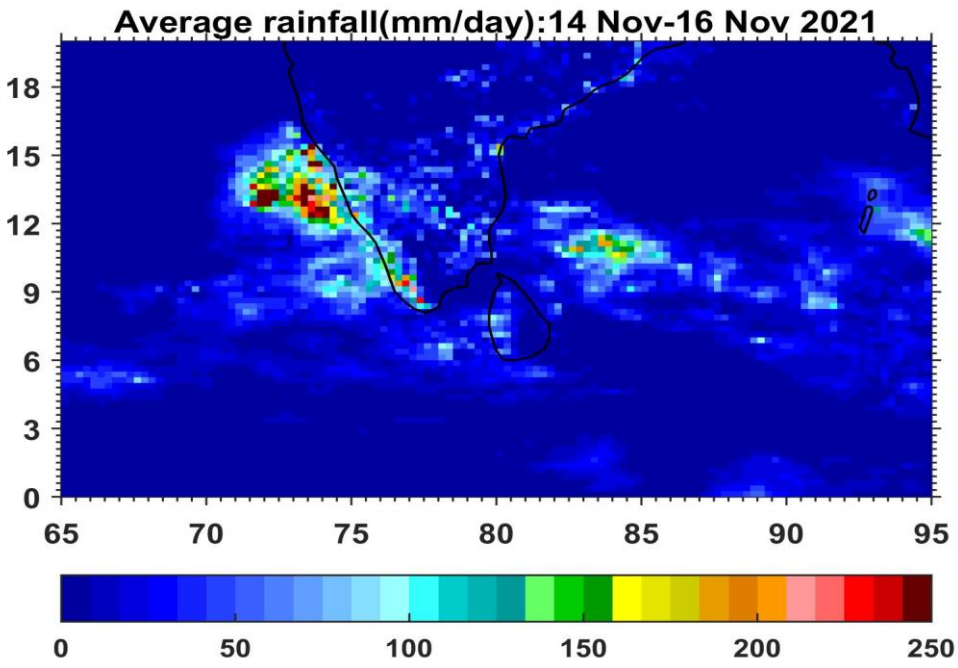

(c)

Fig. 4.2. a) 850 hPa winds on 14 Nov showing the east-west trough (shown as black line) and b) vertical velocity (omega) (Pa/s) at 500 hPa on 14th Nov and c) the cumulative rainfall during 14-16 Nov 2021.

4.2. **Low Pressure Area (LOPAR) : 27 Oct - 04 Nov 2021**

A low pressure formed over the central parts of south Bay of Bengal and associated cyclonic circulation extending up to 5.8 km above mean sea level on 27th Oct 2021. It lay over the southwest Bay of Bengal off Sri Lanka coast and associated cyclonic circulation extended up to 3.1 km above mean sea level on 28th; over southwest Bay of Bengal off Sri Lanka and Tamil Nadu coast and associated cyclonic circulation extended up to 3.1 km on 29th, 30th and 31st. It lay over the Comorin area and adjoining north Sri Lanka coast extending up to 3.1 km on 01st Nov; over the Comorin area and neighborhood on 02nd and over Lakshadweep area and neighborhood extending up to 4.1 km above mean sea level on 03rd and extending up to 4.5 km on 04th Nov 2021.

Various dynamical and thermodynamical features of the LOPAR are shown in Fig. 4.3. The Low pressure area was observed off Sri Lanka Coast with an east-west trough of low pressure from the east Arabian sea to the east Bay of Bengal across the low pressure system. At 925 hPa level, the east-west trough is easily seen. The OLR spatial pattern suggests large scale convection of deep clouds with low OLR (less than 200 Wm^{-2}) over the south peninsula and adjoining Bay of Bengal. The Chennai DWR image as well as the Satellite image are also shown below, which suggests large scale clouding over the region. The cumulative rainfall from 01-04 Nov is shown in Fig. 4.3 c. The spatial pattern suggests heavy rainfall exceeding 200 mm/day off the Tamil Nadu coast. Formation of a low pressure area with associated vertical extension over the seasonal east-west trough of low pressure is a regular synoptic system contributing to seasonal rainfall over the south Peninsula. The present day NWP models have capability in predicting the formation of these low pressure systems over the Bay of Bengal, at least 2-3 days in advance. Therefore, early warnings for adverse weather due to the low pressure systems are feasible.

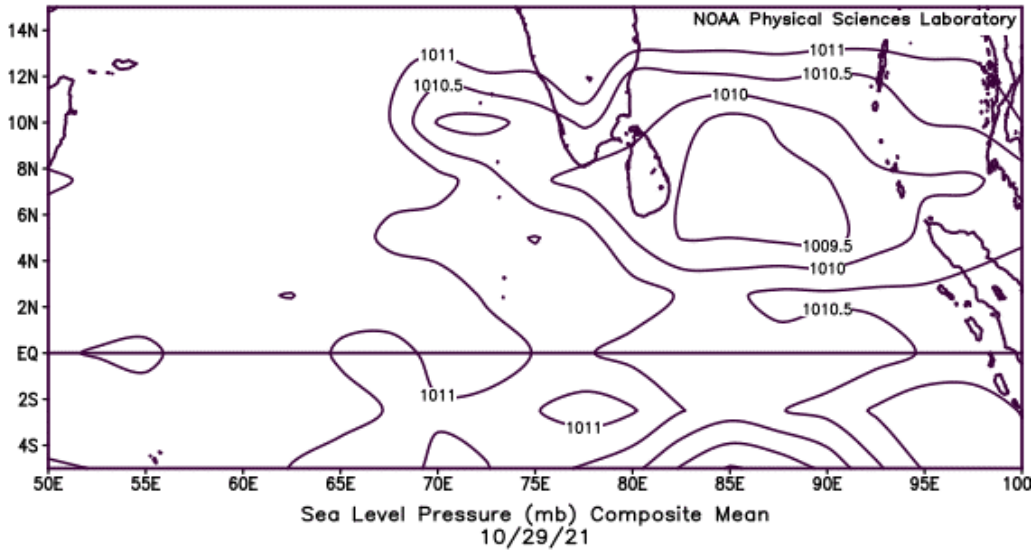

(a)

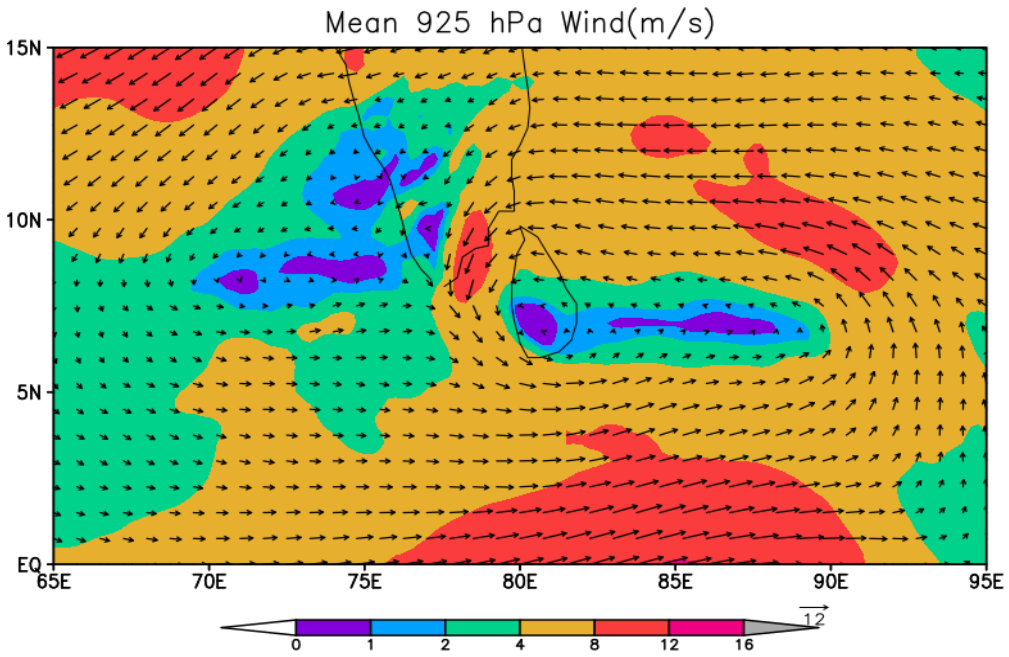

(b)

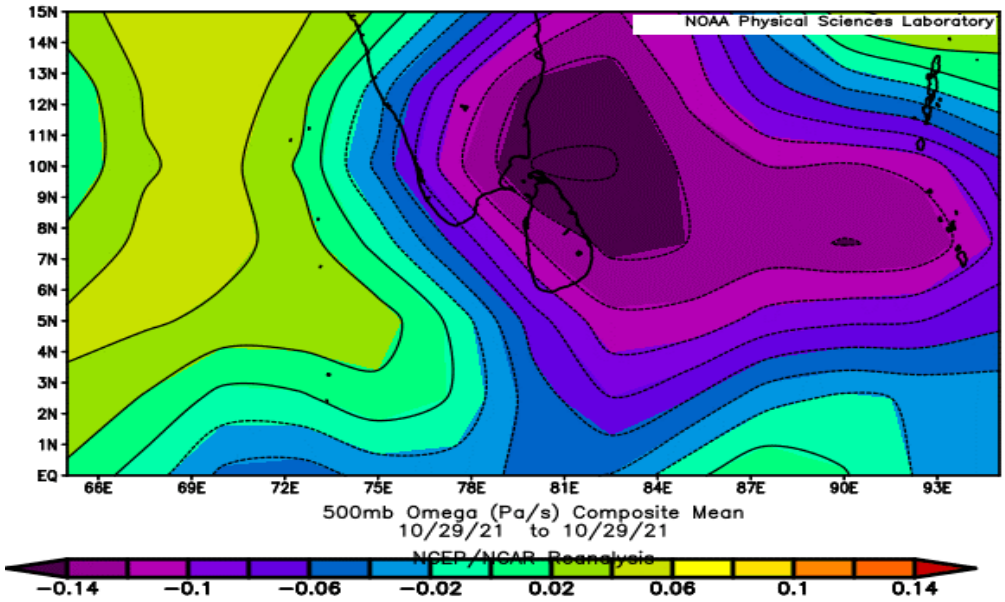

(c)

Fig. 4.3. Various dynamic and thermodynamic features of the LOPAR a) Mean Sea Level Pressure b) 925 hPa winds c) vertical velocity (omega) at 500 hPa on 29 Oct 2021

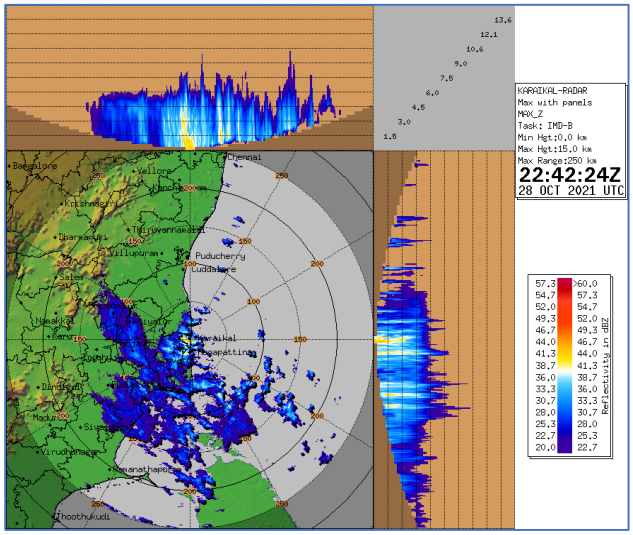

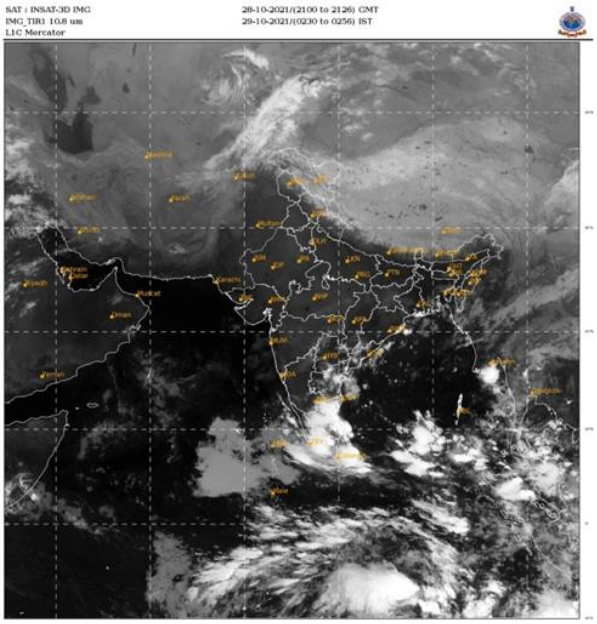

(d) **(e)**

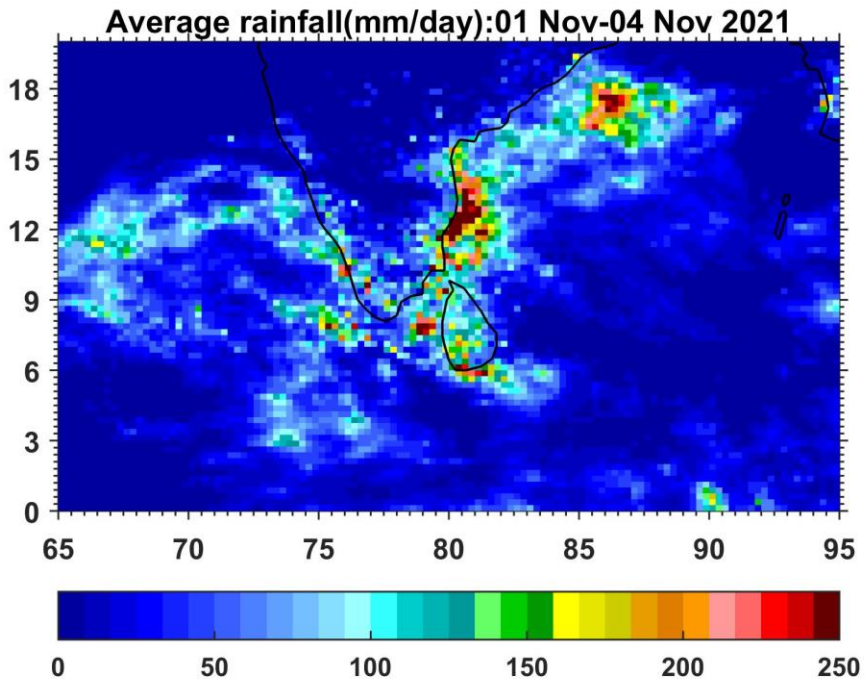

(f)

Fig. 4.3. d) DWR image on 28th Oct e) Satellite Image on 29th Oct and f) Cumulative Rainfall during 01-04 Nov 2021.

4.3. **Cyclonic Storms**

In this section, the details of activity of cyclonic storms are discussed using the long term tropical cyclone track data. Fig 4.4 shows the frequency of Cyclonic Storms (Depressions and above) forming over each 2.5 × 2.5 degree boxes during the period 1961-2020. In each box, top figure shows the frequency of all systems together (Depressions + Cyclonic Storm + Severe Cyclonic Storm), middle one is the frequency of CS+SCS and bottom one is the frequency of SCS alone. These statistics are derived from the IMD Cyclone atlas (http://www.imdchennai.gov.in/). Frequency of cyclonic storms is maximum over the west central Bay of Bengal (10^0-17.5^0N, 80^0-90^0E). Therefore, during the NE monsoon season, north Tamil Nadu and Coastal Andhra Pradesh are most vulnerable to cyclonic storms.

The tracks of cyclonic storms (depressions and above) during the months October to December months are shown in Fig. 4.5, 4.6 and 4.7 respectively. In October, north Tamil Nadu, Coastal Andhra Pradesh, Odisha and West Bengal experience the landfall of these storms. Some storms after moving northwestwards recurve towards northeast, due to the influence of sub-tropical high. Over south Peninsula, north Tamil Nadu and coastal Andhra Pradesh experience Tropical cyclonic storms.

In November, most of the storms forming over the Bay of Bengal move northwestwards and make landfall over Tamil Nadu and the coastal Andhra Pradesh. In November, a few storms recurve and make landfall over West Bengal and Bangladesh. In December, cyclonic storm activity is generally reduced. In December also, when storms form, they move northwestwards and make landfall over Tamil Nadu. A few storms recurve and make landfall over coastal Andhra Pradesh and Bangladesh. There are a few storms, which form over the Bay of Bengal, cross the south peninsula and emerge in the Arabian Sea, thus making longer lifetime. The systems forming over the Arabian Sea, either move westwards towards the Arabian sub-continent or towards Gujarat/Pakistan. The storms forming over the Arabian sea generally do not make

landfall over the south peninsula. They tend move northwestwards. A few storms however move north and affect the Gujarat coasts.

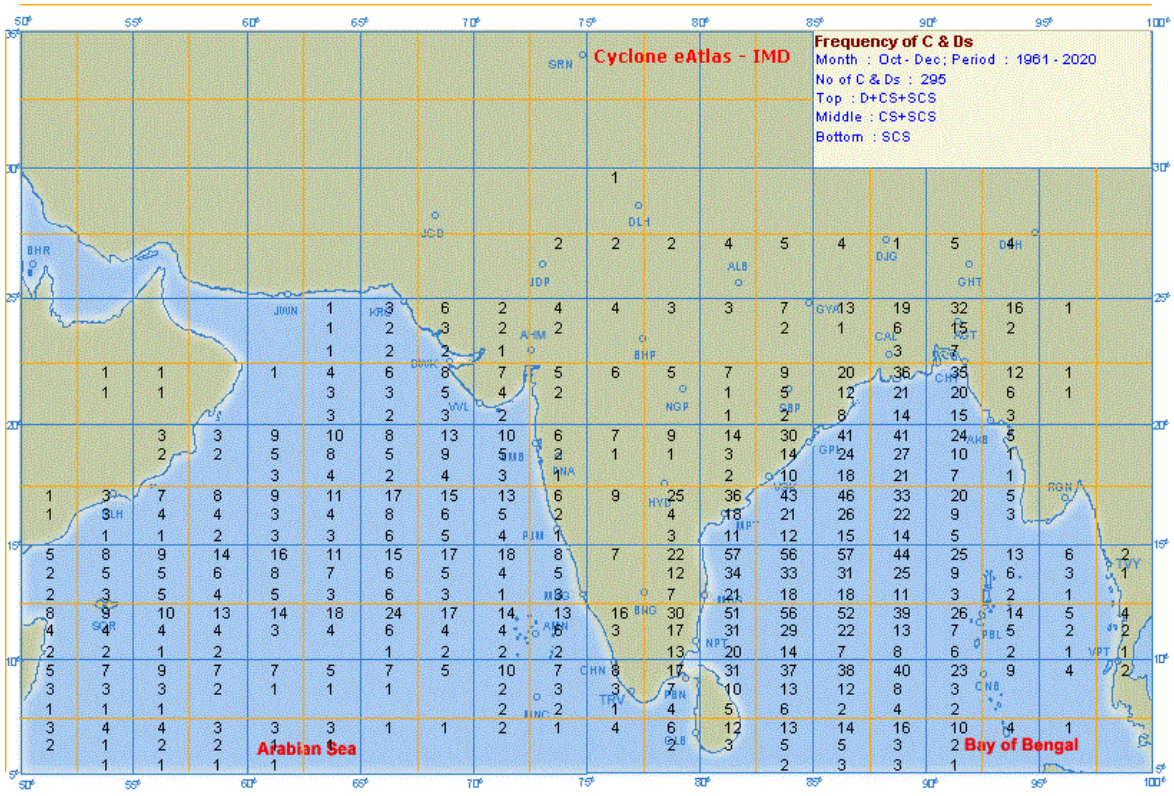

Fig. 4.4. Frequency of all Cyclonic disturbances (Depressions and above) during the period 1961-2020. In each box top figure shows the frequency of Dep+CS+SCS, middle one CS+SCS and bottom one is the frequency of SCS. These statistics is derived from IMD Cyclone atlas.

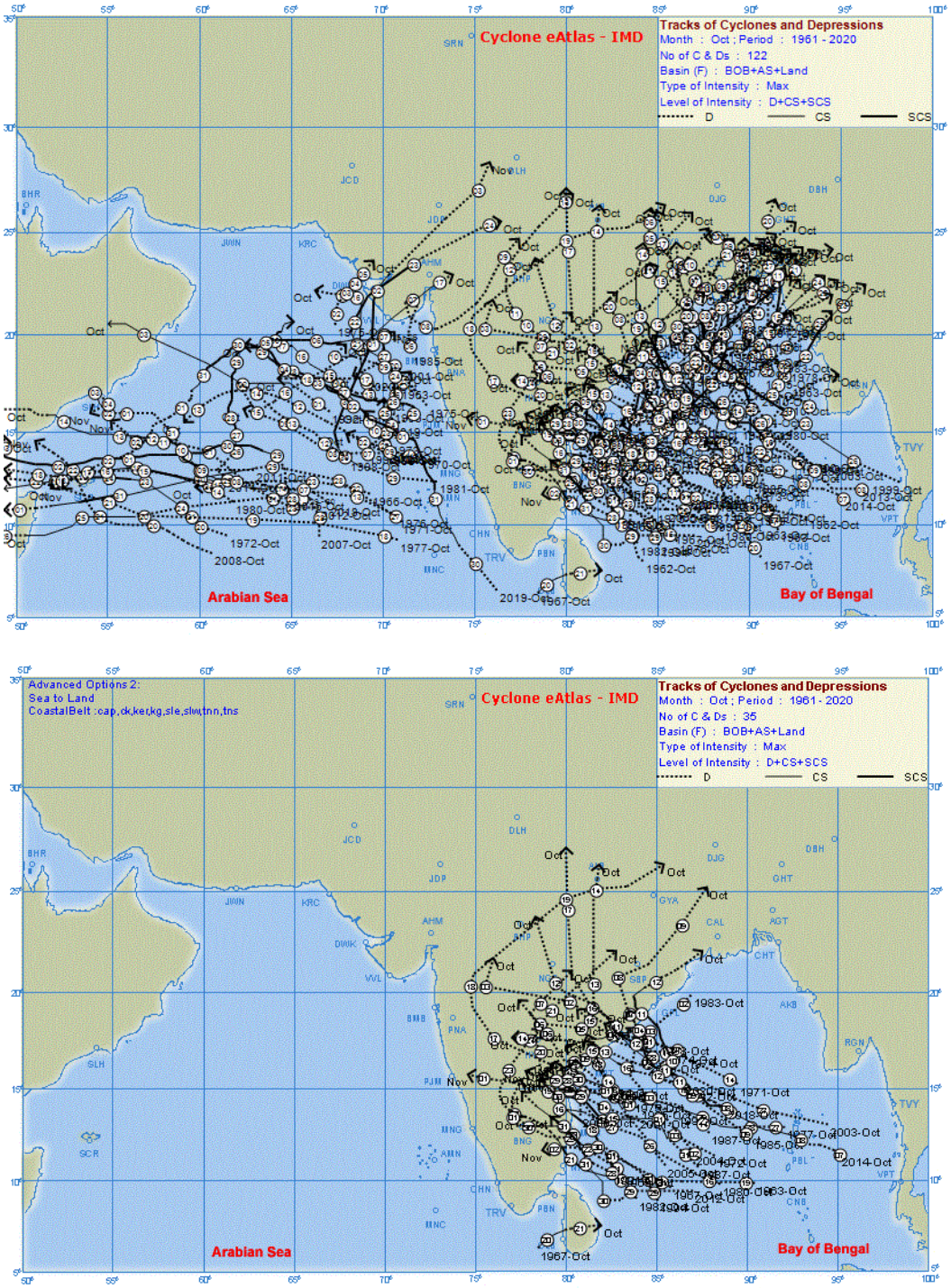

Fig. 4.5. Tracks of cyclonic storms (Depressions and above) during October for the period 1961-2020 (Above) and tracks of cyclonic storms (depressions and above) during October, but which affected the south peninsular region. These tracks are derived from IMD Cyclone Atlas.

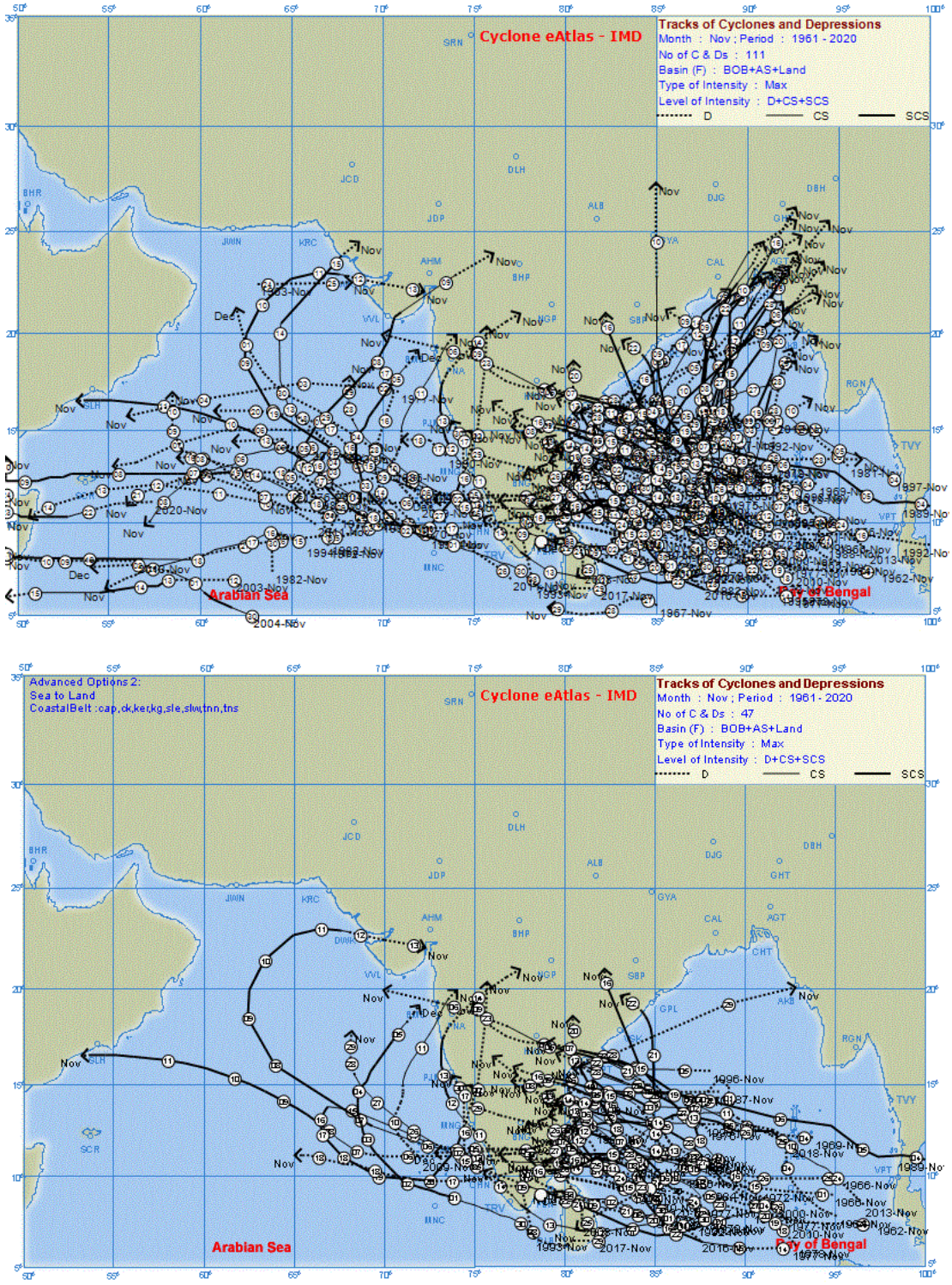

Fig. 4.6. Same as Fig. 4.5, but for November.

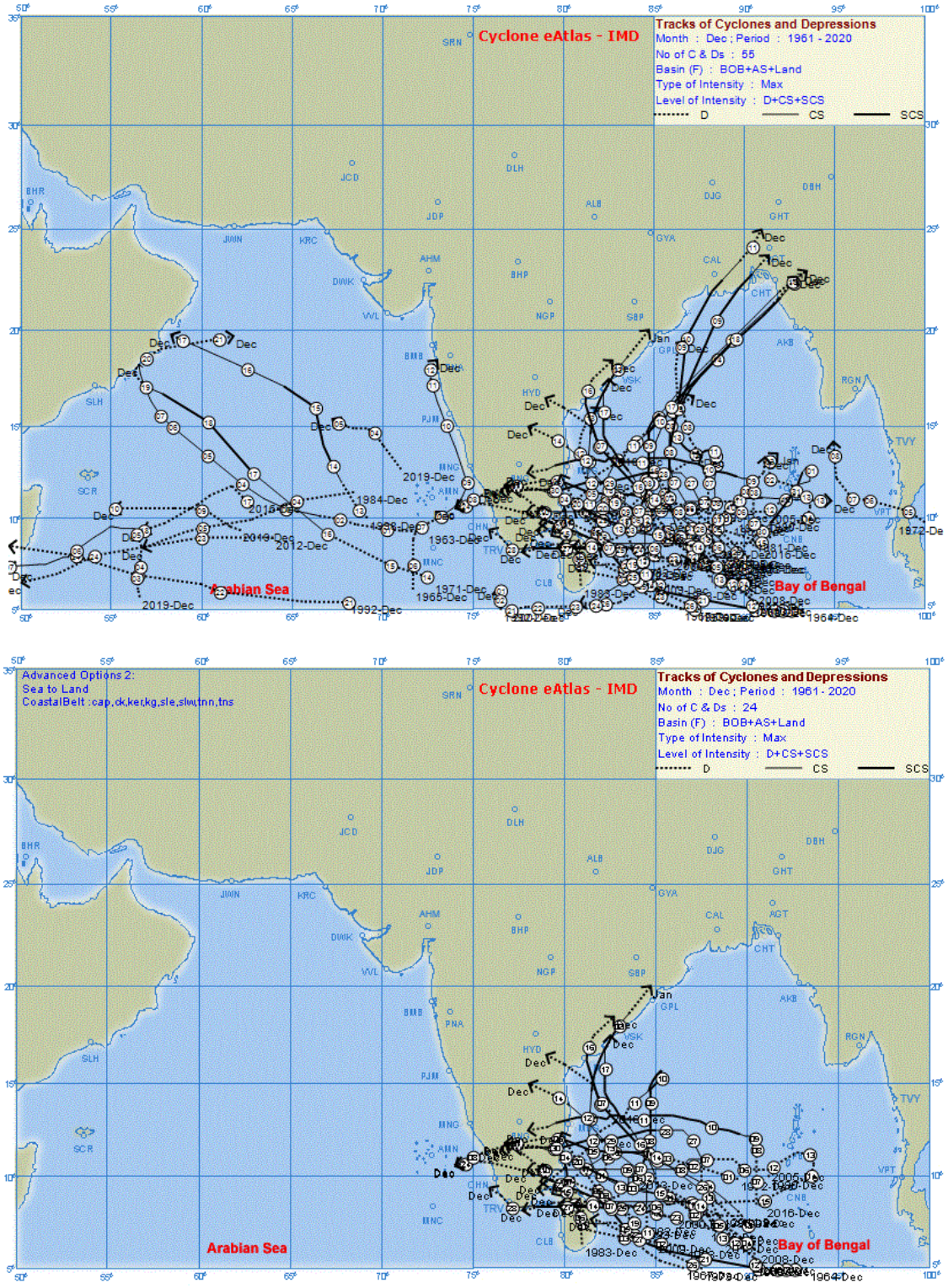

Fig. 4.7. Same as Fig 4.5, but for December.

Figs. 4.8 a, b and c show the return periods (year) of cyclonic storms (CS)/ Severe Cyclonic Storms (SCS) passing within 50 nm of the coastal districts during October, November and December respectively. The period 1961-2020 was considered for this analysis. The maps are derived from the IMD Climate Hazards and Vulnerability Atlas of India, 2022. The same maps for cyclonic storms (CS) and Severe cyclonic storms (SCS) separately are available in the IMD Climate Hazards and Vulnerability Atlas of India (2022). In October, the districts in coastal Andhra Pradesh and north Tamil Nadu have short return periods of 7.5 to 9.0 years. In November, a few coastal districts in south coastal Andhra Pradesh and north Tamil Nadu have much shorter return period of 3.7-5.0 days. Some more neighhouring districts have return periods of 5.1-10.0 years. In December coastal districts of Tamil Nadu show return periods of 7.5-9.0 years.

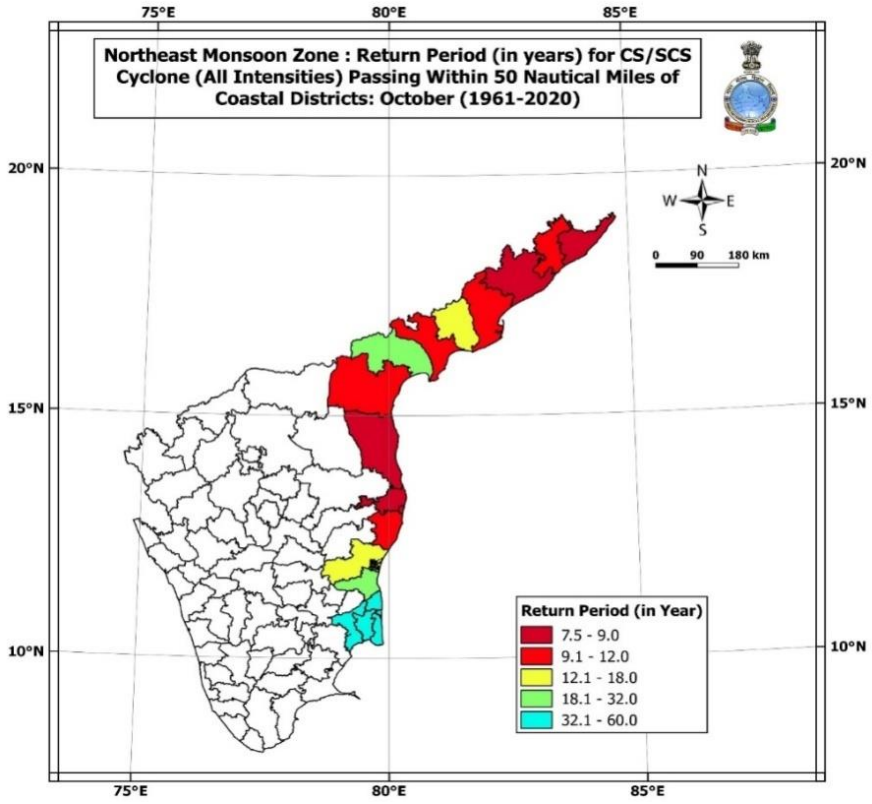

Fig. 4.8 a. Return period (in years) for Cyclonic Storm (CS)/ Severe Cyclonic Storm passing within 50 nautical miles of coastal Districts during October for the period 1961-2020. (Source: IMD Climate Hazards and Vulnerability Atlas of India, 2022).

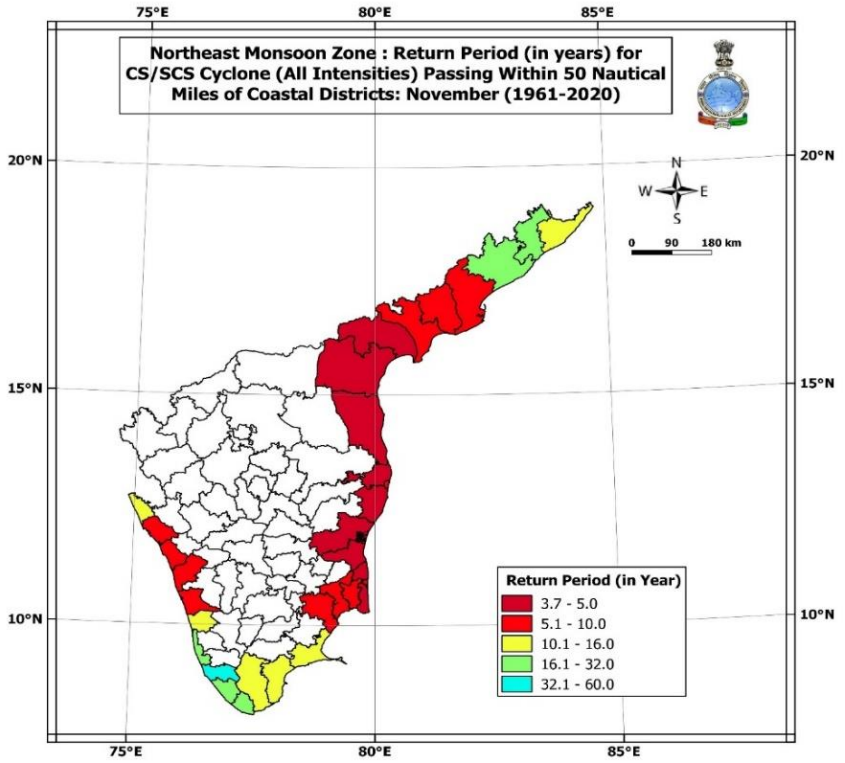

Fig. 4.8 b. Same as Fig 4.5 a, but for November.

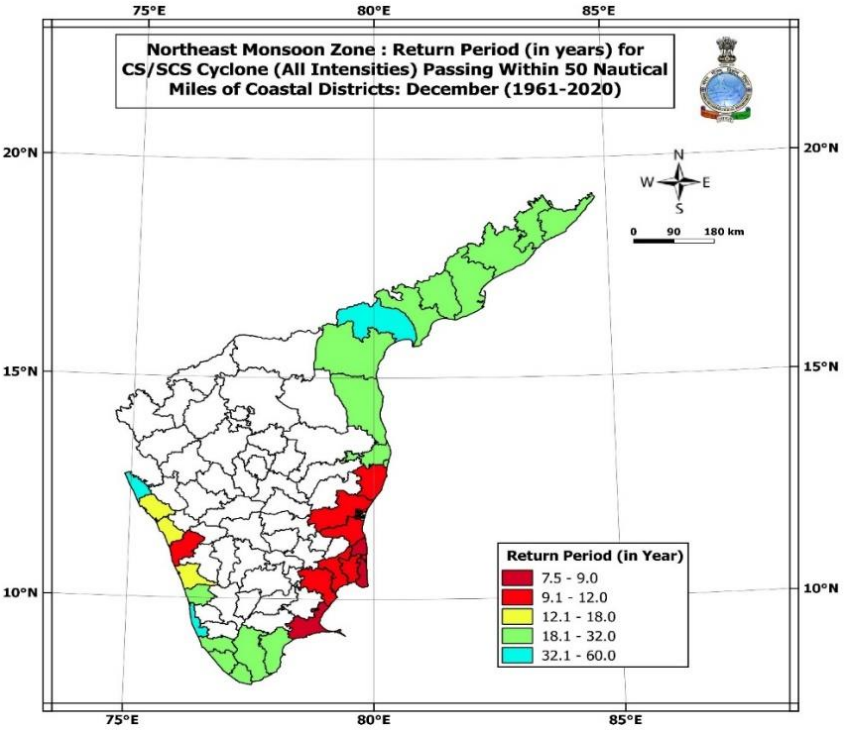

Fig. 4.8 c. Same as Fig 4.5 a, but for December.

4.4. **Track and intensity forecast errors of Tropical Cyclones**

In this section, an analysis is presented on the Track and Intensity forecast errors of Tropical Cyclones over the North Indian Ocean during the NE monsoon (Oct-Dec) season. Data of the period 2012-2021 have been used to complete this analysis. Mohapatra et al. (2013) and Mohapatra et al. (2015) have carried out extensive analysis of tropical cyclone track forecast errors over the North Indian Ocean.

The comparative analysis of track and intensity forecast errors for the post monsoon season (October-December) during 2017-21 and 2012-16 are presented in Fig. 4.9 a and b respectively. The track forecast errors were 82 km, 107 km, 139 km & 272 km during the period 2017-21 for the 24, 48, 72 & 120 hours lead forecasts respectively. However, during the period 2012-2016, the corresponding errors were 88 km, 133 km, 185 km & 348 km. It indicates an improvement of 10% in track forecast errors for lead period up to 24 hours and 15-20% for lead period beyond that up to 120 hours (Fig. 4.9 a) during the recent years.

The intensity forecast errors were 8.1 knots, 11.7 knots, 14.2 knots & 15.8 knots during 2017-21 for 24, 48, 72 & 120 hours lead period respectively. The corresponding errors during the period 2012-2016 were 11.9 knots, 16.9 knots, 17.2 knots & 11.6 knots respectively. The intensity of a tropical cyclone is measured based on its maximum wind which is normally quoted in knots. This indicates an improvement of 30% in intensity forecast errors for lead period up to 48 hours and 15-25% for lead period of 60 to 84 hours (Fig. 4.9 b).

To carry out the analysis of landfall errors, only landfalling cyclones have been considered. There were 9 cyclones in each period making landfall over different places within the region during the NE monsoon season. The comparative analysis of landfall point forecast errors for the NE monsoon season during 2017-21 and 2012-16 are presented in Fig. 4.9 c. The landfall point forecast errors were 41.9 km, 59.3 km & 51.2 km during 2017-21 against 31.6 km, 85.3 km & 82.7 km during 2012-2016 for 24, 48 &

72 hours lead period respectively. The comparative analysis indicates that there is a significant improvement of 30-40% in landfall point forecast errors for lead period of 48-96 hours. However, there is no significant change in landfall point forecast errors up to a lead period of 36 hours during the two periods. It is needless to mention here that the diameter of the central region (eye) of the TC is about 10-100 km, and an average about 50 km. No significant change in the forecast errors up to 36 hours which vary from about 15-60 km can be attributed to the above fact. Further within 36 hours, the landfalling TCs are monitored with the help of the coastal hourly observations as well as Doppler weather radar observations, leading to lower detection error. It is very interesting to note that the landfall forecast errors during the recent epoch are much less than the previous epoch. This could be mainly attributed to the excellent modelling strategy used by the IMD; availability of global models with higher resolution with plenty of assimilated data. The global models used for predicting the track and the landfall point have the spatial resolution of about 12-25 km. Hence, there is scope to reduce the landfall point errors for higher lead periods like 48-120 hours with improvement in model resolution, data assimilation supported by augmented direct & remotely sensed observational system.

Cangialosi et al. (2020) have discussed the Hurricane forecast errors over the Atlantic Ocean since 1960s to 2019. It has been well documented that the National Hurricane Center (NHC) has made significant improvements in Atlantic basin tropical cyclone (TC) track forecasting during the past half century. In contrast, NHC's TC intensity forecast errors changed little from the 1970s to the early 2000s. Recently, however, there has been a notable decrease in TC intensity forecast error and an increase in intensity forecast skill. The advancement of NWP models, especially as supported in the past decade, creation of the consensus aids, development of rapid intensification guidance, and the ability of the NHC forecasters to add value to the TC guidance has greatly improved intensity forecast skill over the Atlantic Ocean.

The study by Cangialosi et al. (2020) revealed that the track forecast errors over the Atlantic Ocean during the period 2010-2019 are 83 km, 110 km, 185 km and 213 km respectively for 24 hr, 48 hr, 72 hr and 120 hr forecasts. Similarly for Hurricane Intensity forecasts the errors are 8 knots, 12 knots, 14 knots and 15 knots respectively for 24 hr, 48 hr, 72 hr and 120 hr forecasts during the same period. This suggests, the tropical cyclone forecast intensity errors over the North Indian Ocean are larger compared to the intensity forecasts errors for the Atlantic Ocean. Therefore, more efforts should be made to reduce track and intensity forecast errors of tropical cyclones over the North Indian Ocean.

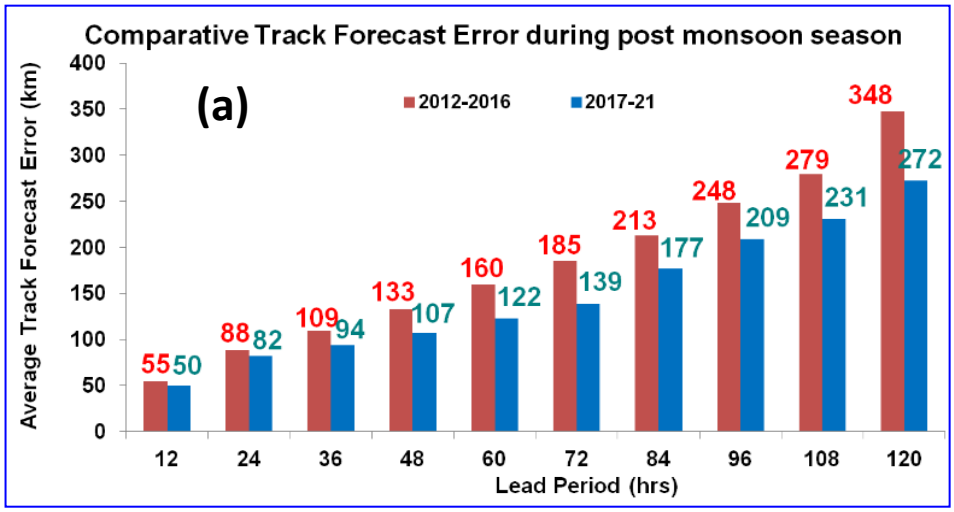

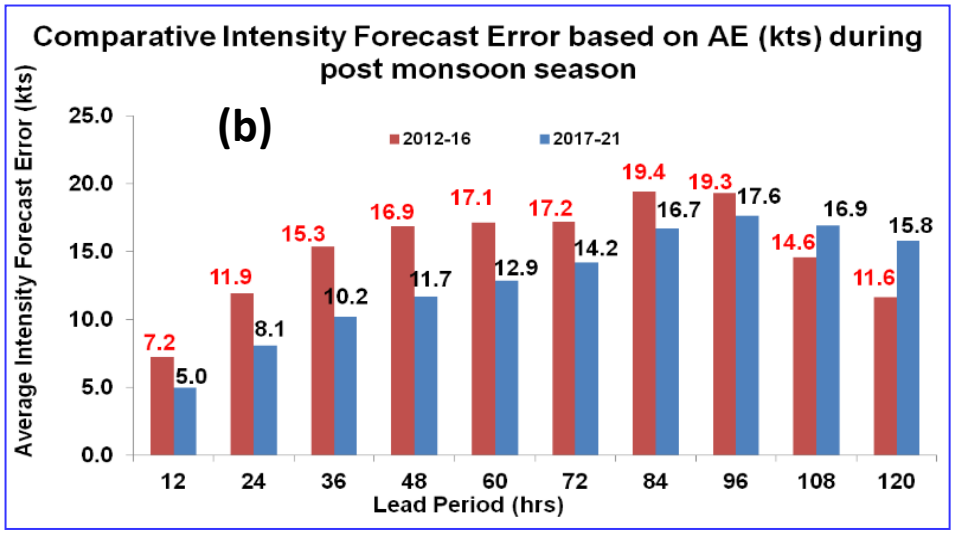

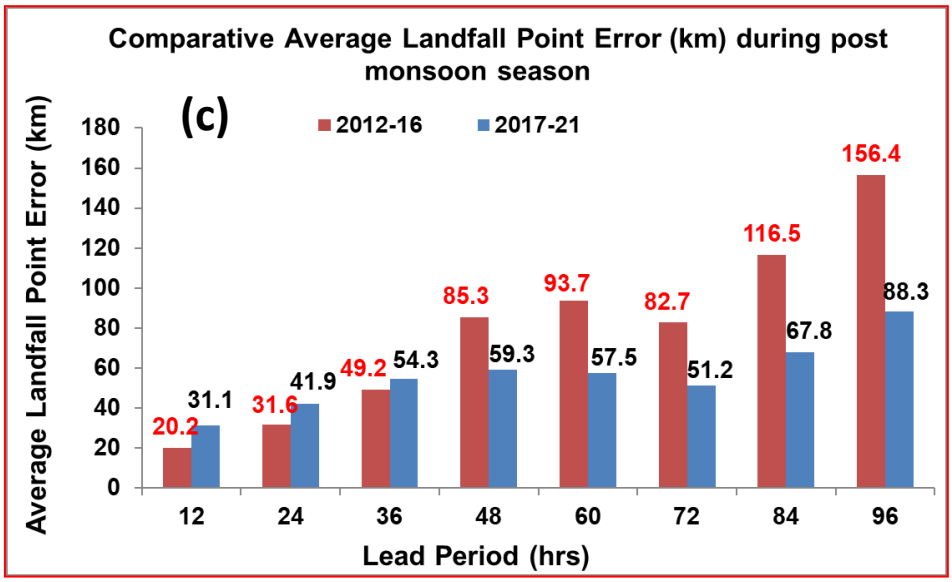

Fig. 4.9. Comparative operational (a) track and (b) intensity and (c) Landfall forecast in the post monsoon season during 2017-21 against 2012-16**.**

4.5. **A case study of Tropical Cyclone Ockhi**

In this section, the details of the tropical cyclone (TC-OCKHI) are discussed to bring out various forecasting issues and challenges related to the cyclone during the NE monsoon season. The TC- Ockhi was responsible for deaths of over 350 people from southern Tamil Nadu and Kerala, between 30 Nov and 3 Dec 2017. There were also some unidentified fishers from the north-eastern states of India who were lost at sea while working on-board fishing vessels. The full force of the storm was borne by fishermen at sea, unlike the previous cyclones over the Arabian sea (Manas Roshan 2019).

The TC OCKHI formed as a low pressure area over southwest Bay of Bengal (BOB) and adjoining areas of south Sri Lanka on 28th Nov /0300 UTC and became well marked on 29th /0000 UTC over the same region. The vertical wind shear of horizontal wind was moderate to high (15-30 knots) over the southwest Bay of Bengal and adjoining Sri Lanka coast. Under the favourable environmental conditions, it concentrated into a Depression (D) over southwest BOB off southeast Sri Lanka coast on 29th / 0300 UTC.

Moving westwards, it crossed Sri Lanka and emerged into Comorin area by 29th /1200 UTC. It intensified into a Deep Depression (DD) on 29th/2100 UTC. Moving northwestwards it intensified into a Cyclonic Storm (CS) on 30th / 0300 UTC over the Comorin area, into a Severe Cyclonic Storm (SCS) over Lakshadweep area on 01st December / 0000 UTC and further into a Very Severe Cyclonic Storm over southeast Arabian Sea (AS) to the west of Lakshadweep by 01st / 0900 UTC.

Generally, for the North Indian Ocean basin, TCs are considered to have undergone rapid intensification (RI)/ rapid weakening (RW) whenever 30 knots increase/decrease is noted in maximum sustained surface wind speed (MWS; Vmax) in 24 hrs. It is interesting to note that OCKHI underwent RI between 01st /0000 UTC to 02nd 0000 UTC and attained its peak intensity of 150-160 kmph gusting to 180 kmph on 2nd /0900 UTC with lowest central pressure of 976 hPa over the Arabian Sea. It then gradually recurved north-northeastwards, maintained its VSCS intensity till 04th / 1200 UTC and then weakened gradually. It crossed the south Gujarat coast as a well-marked low on 06th Dec/0000 UTC (IMD, 2018). More details of its genesis and tracks are available in Geetha and Balachandran (2020) and the IMD (2018) report on TC-Ockhi (https://rsmcnewdelhi.imd.gov.in/uploads/report/26/26_83ec45_ockhi%20pre.pdf).

The system caused extensive damages over extreme south Tamil Nadu and south Kerala during its developmental stages on 29-30 Nov. The system centre was about 60 km from Kanyakumari, the southern-most tip of peninsular India on 30th Nov/ 0300 UTC when it intensified from DD to CS stage (as per IMD's best track data). Even though the centre of the system did not cross the coast and move inland, Kanyakumari and Thiruvananthapuram (Kerala) bore the brunt of the fury of the eye-wall region of the TC during 29th night-30th Nov morning. The IMD's best track of TC-OCKHi is shown in Fig. 4.10 and spatial pattern of mean sea level pressure on 29th Nov and 30th Nov is shown in Fig. 4.11. These charts show the movement of TC-OCKHI and quick intensification by 30th Nov near the Comorin area.

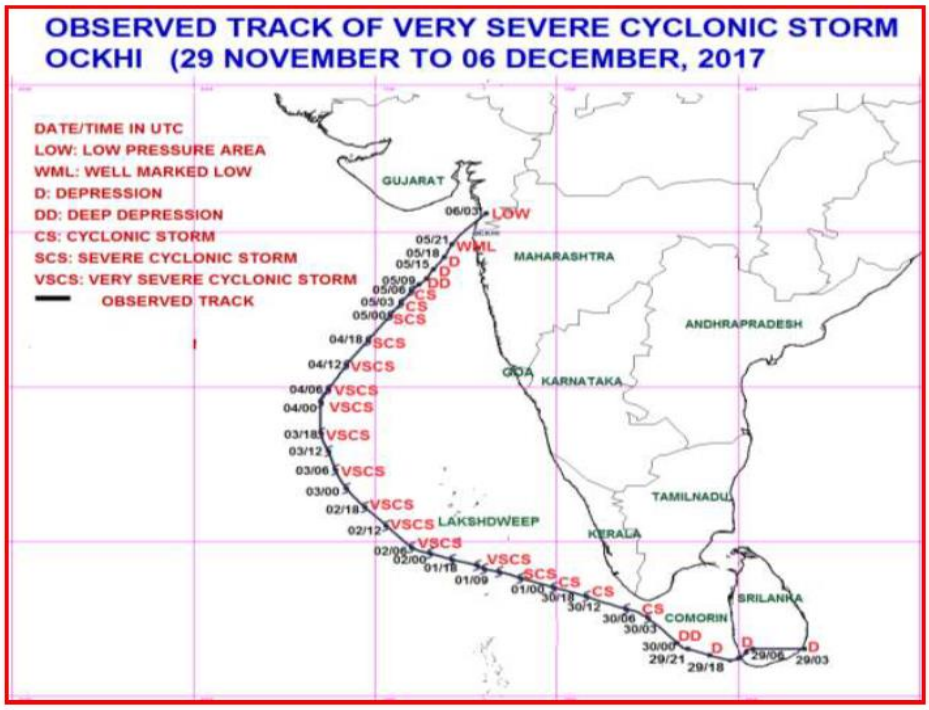

Fig. 4.10. Observed track of very severe cyclonic storm OCKHI, 29 Nov to 06 Dec 2017. Source: India Meteorological Department (IMD).

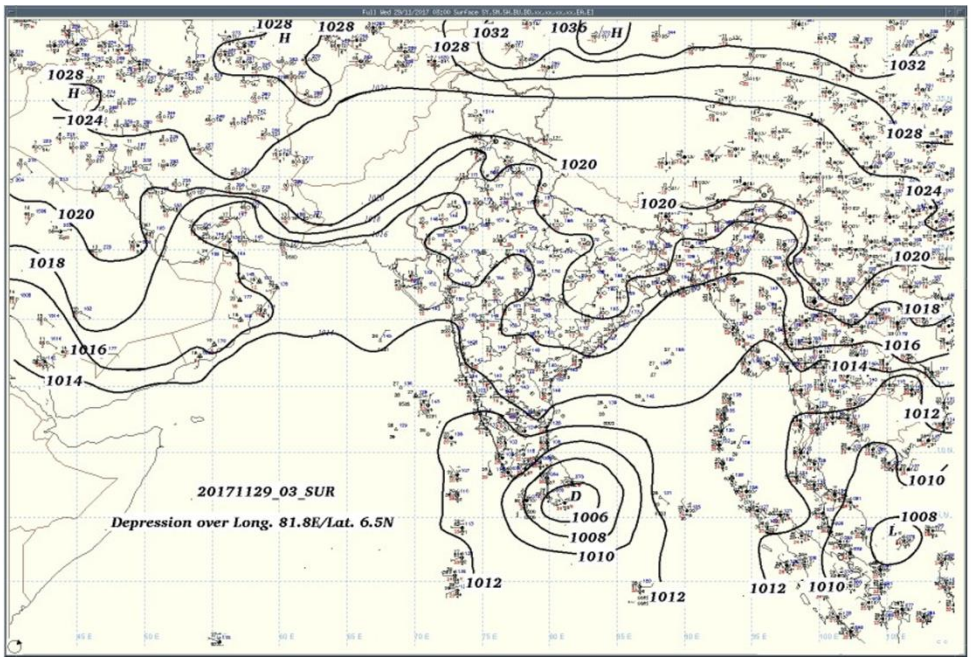

(a)

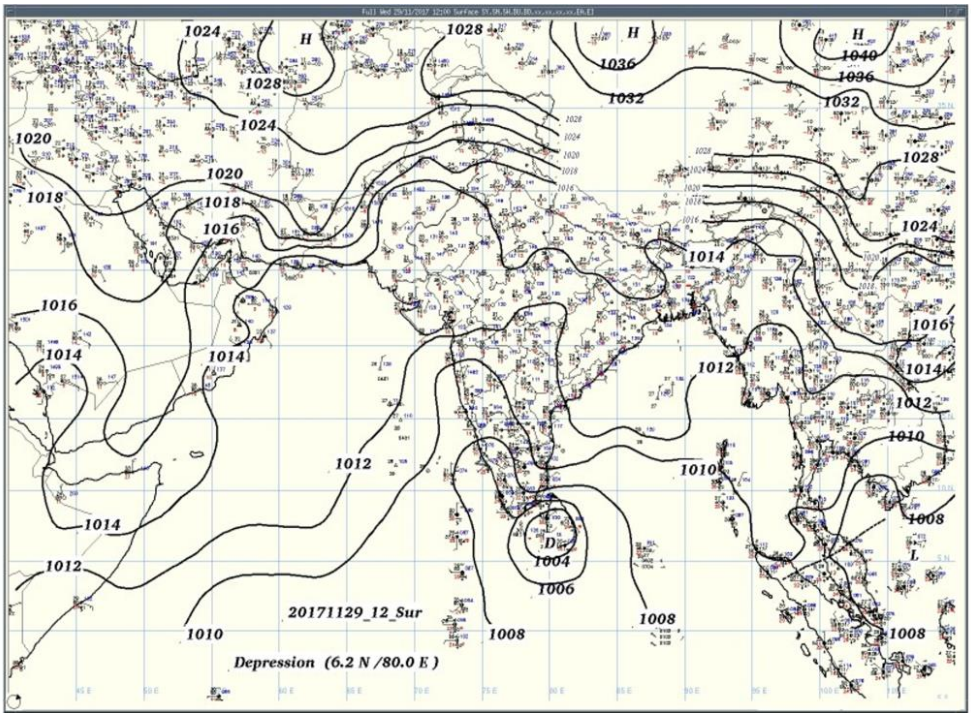

(b)

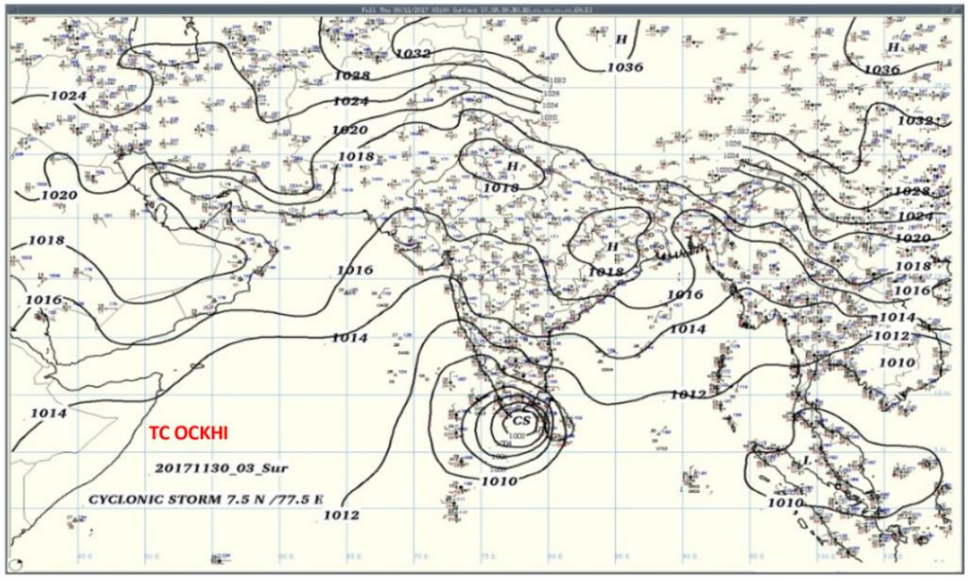

(C)

Fig. 4. 11. Mean Sea Level Pressure Chart on a) 29 Nov 2017, 03 UTC b) 29 Nov 2017 12 UTC and c) 30 Nov 2017 03 UTC. Source: India Meteorological Department.

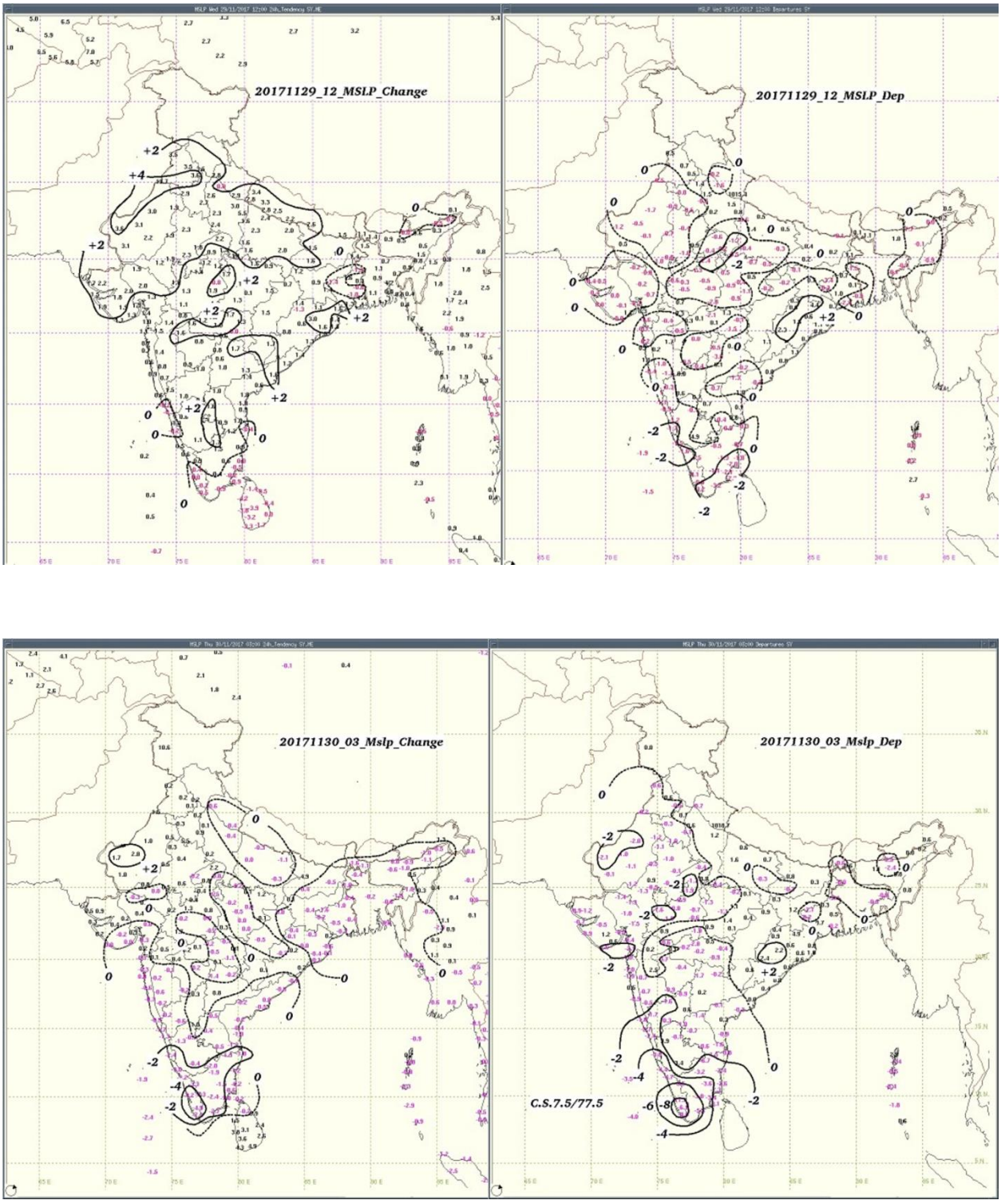

Fig. 4.12. 24 hour change in MSLP (on left) and MSLP departure from normal (right) on a) 29th Nov 2017 12 UTC and b) 30th Nov 2017 03 UTC. Source: IMD Meteorological Department.

Fig. 4.12 above shows the Mean Sea Level Pressure (MSLP) changes in 24 hour and MSLP departures from normal on 29th and 30th Nov 2021. These charts show rapid fall of mean sea level pressure by 30th Nov and large-scale negative departure (of the order of 8 hPa) off the Kerala coast.

Fig. 4.13 shows low level convergence and 850 hPa vorticity patterns at 03 and 12 UTC on 29th Nov, when the system intensified into a cyclonic storm. The low-level convergence pattern shows a rapid increase in the low-level convergence over the region associated with the weather system. The INSAT satellite pictures of TC-Ockhi are shown in Fig. 4.14. These images are provided by the Satellite Directorate of IMD, which shows the westward movement and then north-northeasterly recurvature towards the Gujarat coast.

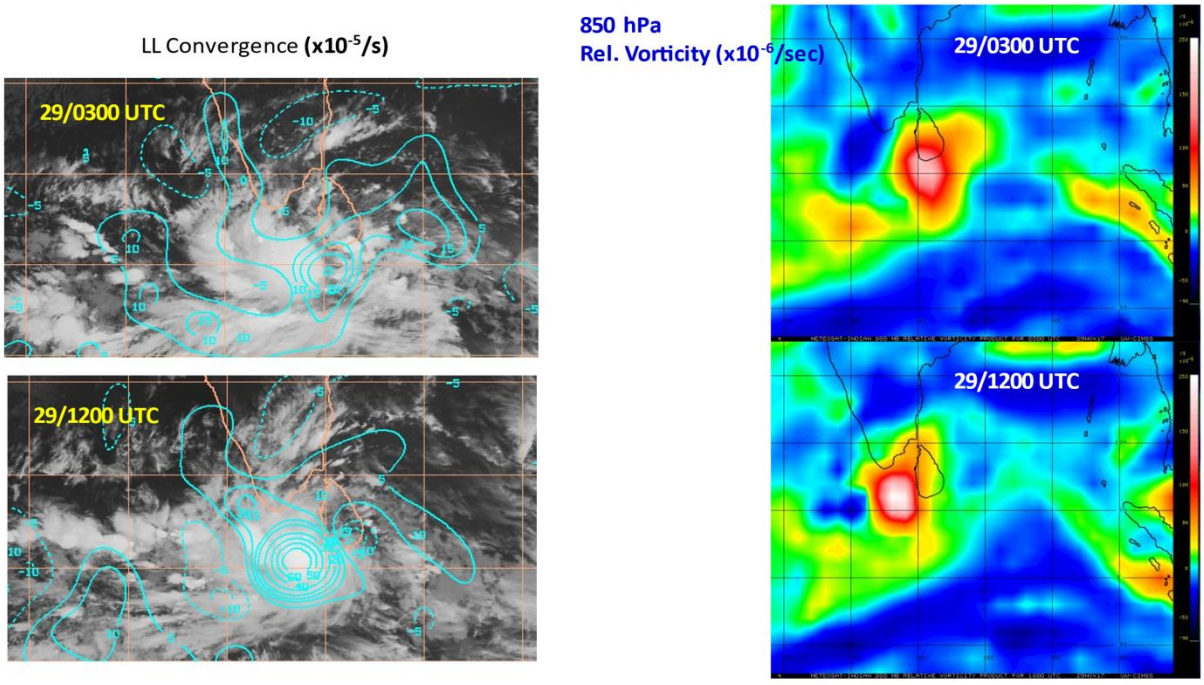

Fig. 4.13. Low-level convergence (10^{-5}/s) (left) and 850 hPa vorticity (10^{-5}/s) (right) at 03 and 12 UTC on 29th Nov 2017. Source: IMD

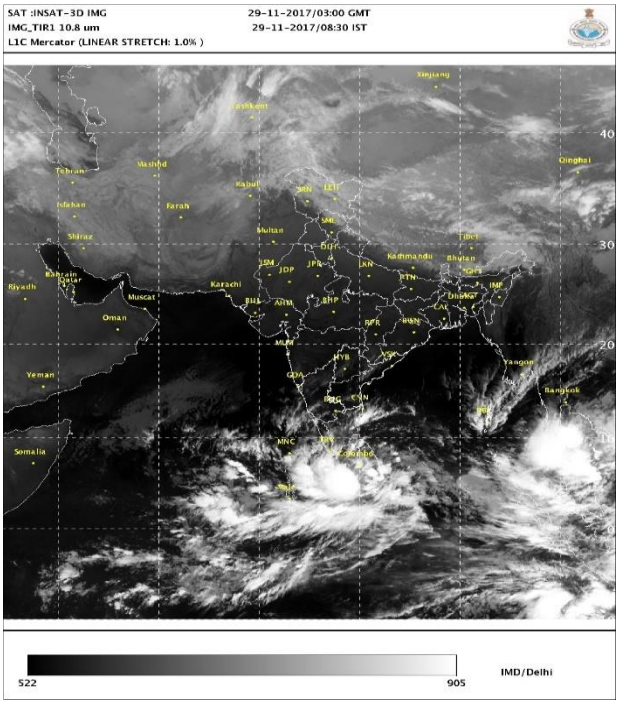

a) 29 Nov 0300 UTC

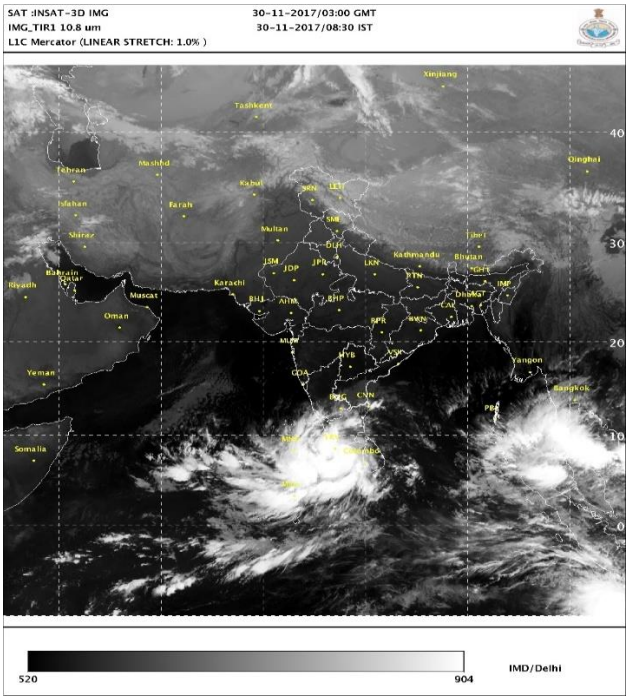

b) 30 Nov 0300 UTC

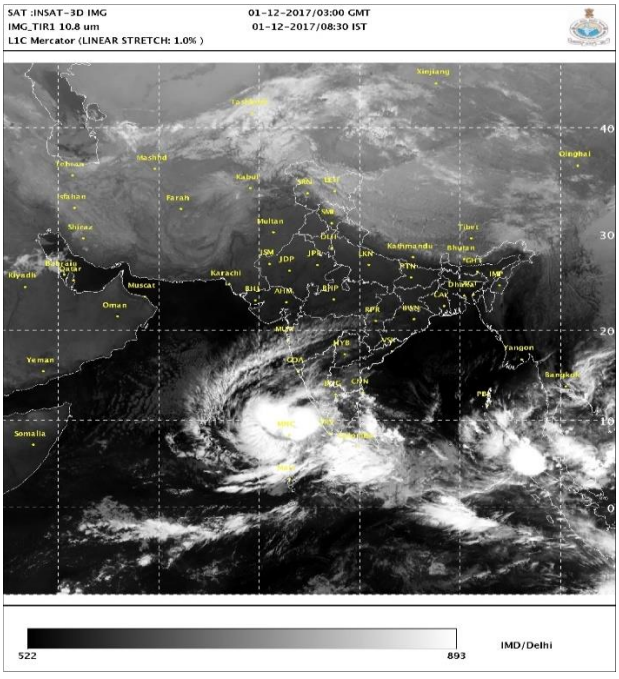

c) 01 Dec 0300 UTC

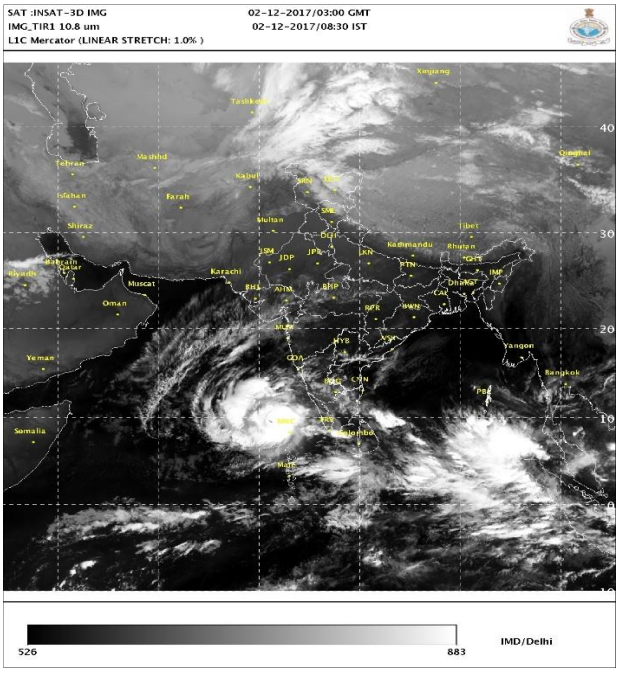

d) 02 Dec 0300 UTC

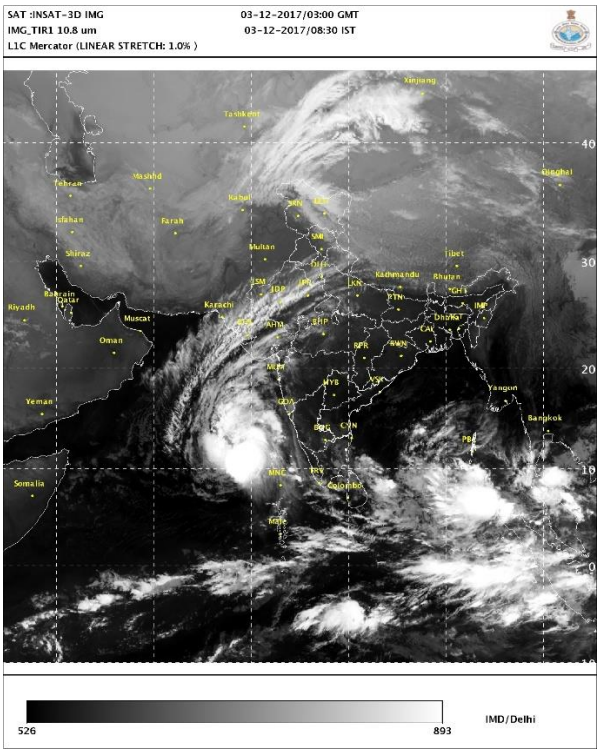

e) 03 Dec 0300 UTC

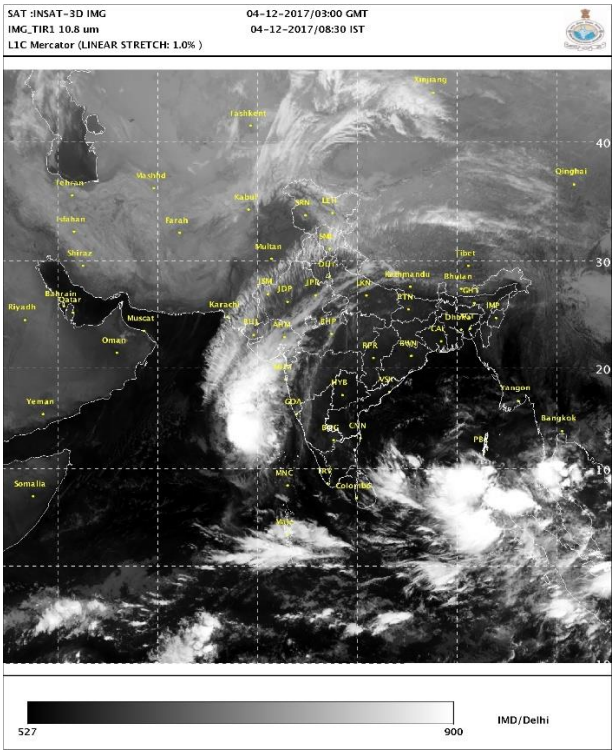

f) 04 Dec 0300 UTC

Fig. 4.14. INSAT IR image at 0300 UTC showing TC-Ockhi during 29 Nov- 04 Dec 2017. Source: IMD Satellite Directorate.

Fig. 4.15 shows the spatial distribution of 10 m wind (in knots) from 29 Nov to 4th Dec showing the intensification and weakening of surface winds associated with TC-Ockhi. These plots are prepared using the ERA5 reanalysis data with 0.25 degree resolution.

It caused heavy to very heavy rainfall over Lakshadweep on 01st and 2nd Dec. There was heavy rainfall over north coastal Maharashtra and adjoining south coastal Gujarat on 5th Dec. Thiruvananthapuram recorded 62 kmph wind in gustiness at 1300 IST of 30th Nov. Storm surge of height 1m over Lakshadweep Islands was observed on 30th Nov.

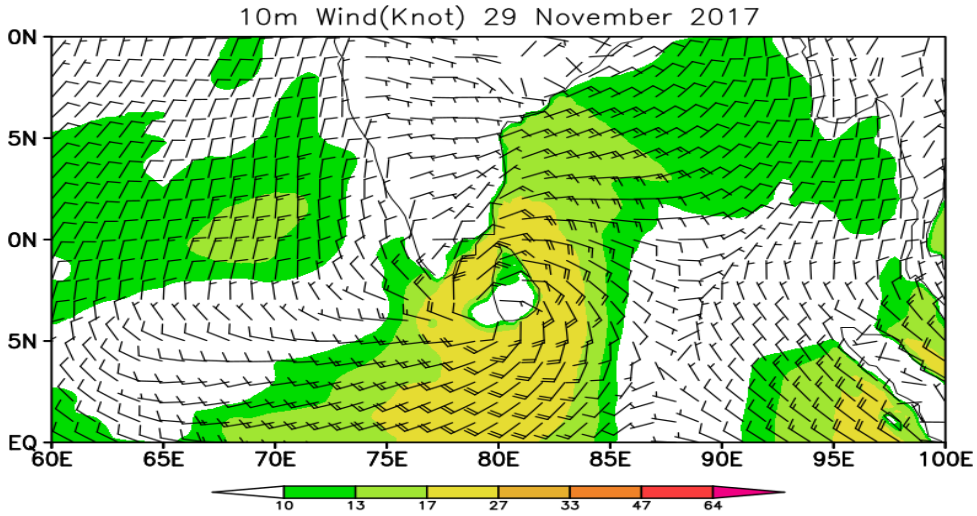
10m Wind(Knot) 29 November 2017
0N
5N
0N
5N
EQ
60E
65E
70E
75E
80E
85E
90E
95E
100E
10
13
17
27
33
47
64

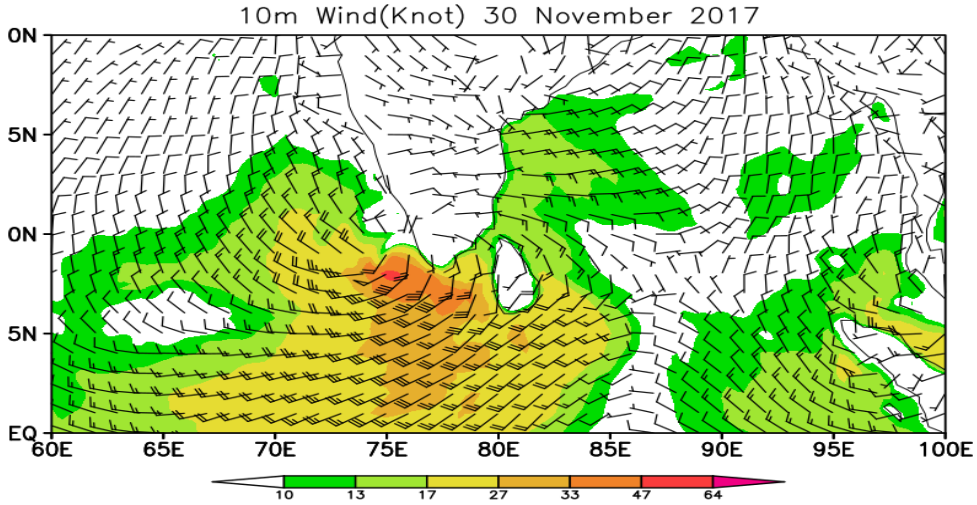
10m Wind(Knot) 30 November 2017
0N
5N
0N
5N
EQ
60E
65E
70E
75E
80E
85E
90E
95E
100E
10
13
17
27
33
47
64

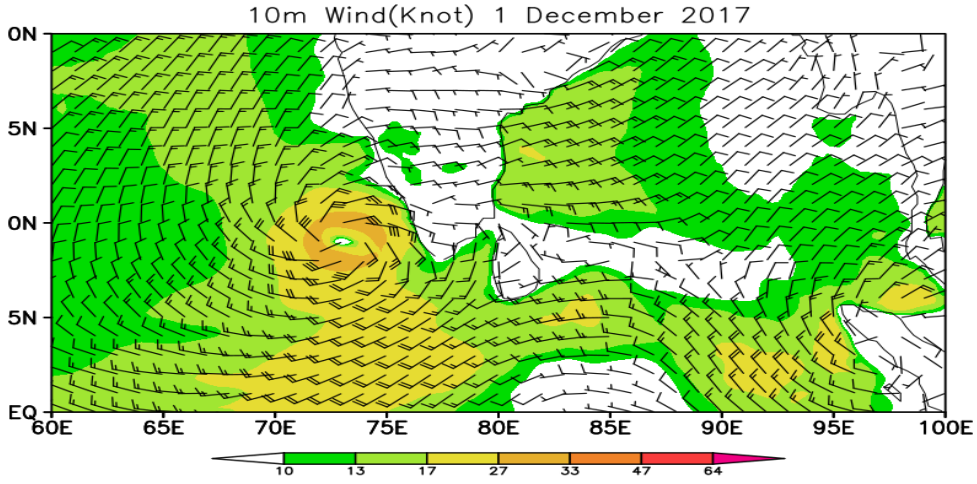
10m Wind(Knot) 1 December 2017
0N
5N
0N
5N
EQ
60E
65E
70E
75E
80E
85E
90E
95E
100E
10
13
17
27
33
47
64

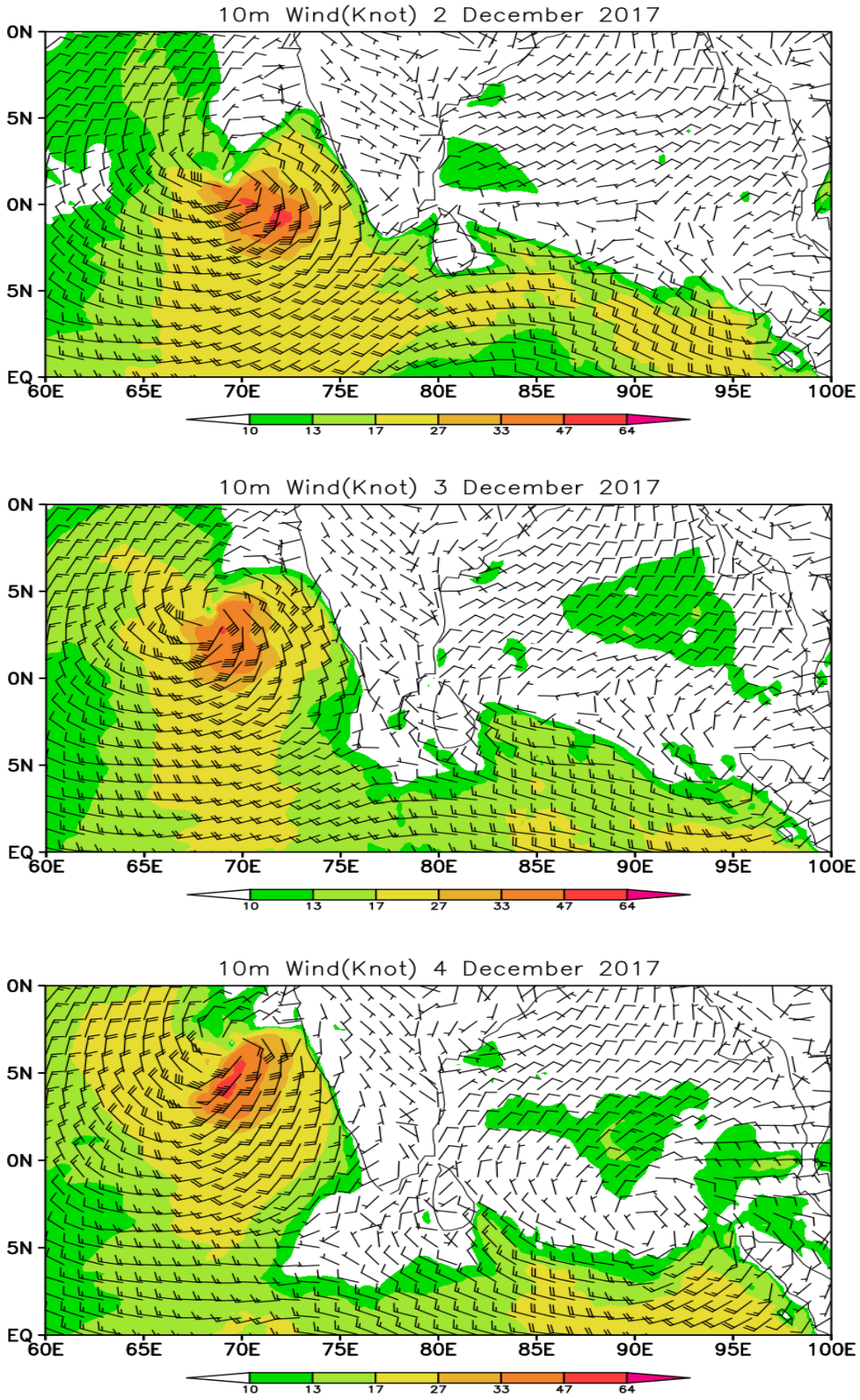

Fig. 4.15. Spatial distribution of 10 m wind in knots from 29 Nov to 4 Dec 2017. Source: ERA reanalysis data

The salient features of TC-Ockhi are given below (IMD, 2018):

- This was the only fourth cyclonic storm developing over the Comorin Sea (south of Kerala and Tamil Nadu and west of Sri Lanka) during the past 120 years. Previously two cyclones (19-22 Nov and 17-19 Dec) in 1912 and another in 1925 (06-10 Nov) developed over the Comorin Area. All these cyclones affected south Kerala and south Tamil Nadu.
- TC-Ockhi was thus a rare cyclone with rapid intensification in genesis stage (from depression to cyclonic storm within 24 hours). The system intensified rapidly from 1800 UTC of 30th to 0000 UTC of 2nd Dec (increase in wind speed by 30 kts in 24 hours) (Fig. 4.16).
- The total track length of the cyclone was 2538 km.
- The 12 hourly average translational speed of the cyclone was 15.0 kmph. However, it moved faster in the genesis stage (29/0830 IST to 30/0830 IST) with 12 hourly average translational speed of 19 kmph.
- The life period of cyclone was 6 days & 18 hours against long period average of 4.7 days for very severe cyclonic storm over north Indian Ocean.
- The peak maximum sustained surface wind speed (MSW) of the cyclone was 150-160 kmph gusting to 175 kmph (85 knots) during 0600 UTC of 2nd to 0000 UTC of 3rd December (Fig. 4.17)
- The lowest estimated central pressure was 976 hPa (from 0300 UTC of 2nd to 0000 UTC of 3rd December) with a pressure drop of 34 hPa (Fig. 4.17).
- The intensification/weakening of TC-Ockhi was largely governed by the Ocean heat content. However, the rapid weakening on 4th and 5th Dec was facilitated by dry and cold air intrusion and high vertical wind shear under the influence of a trough in mid latitude westerlies.

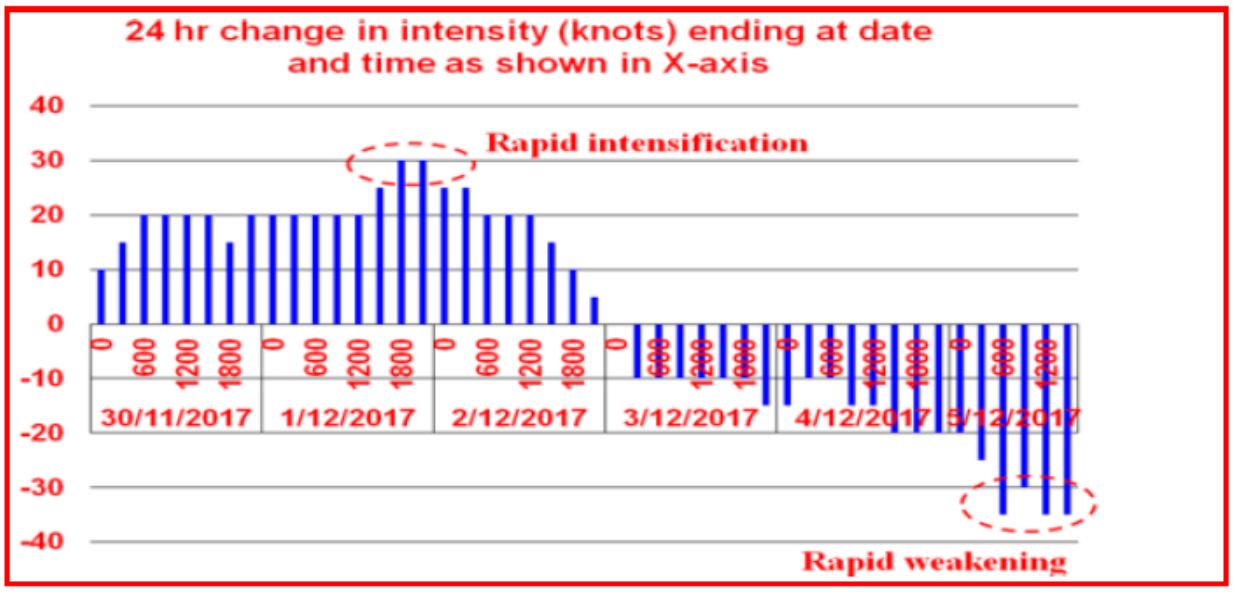

Fig. 4.16. 24-hour change in intensity (knots) ending on different date and time. Rapid intensification and rapid weakening are indicated. Source: IMD 2018 report.

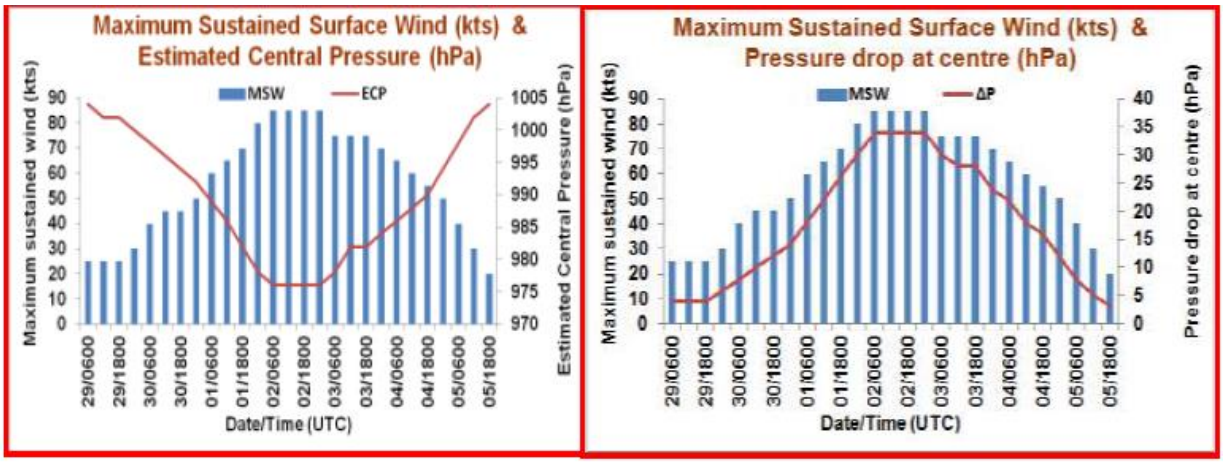

Fig. 4.17. a) Maximum sustained surface wind (kts) and estimated centre pressure (hPa) and b) Maximum sustained surface wind (kts) and pressure drop at centre (hPa). Source: IMD 2018 report.

Genesis and intensification of tropical cyclones are closely related to oceanic conditions like sea surface temperatures (SST) and ocean heat content. Fig. 4.18 shows the spatial distribution of SST during 23-28 Nov, just prior to the formation of TC-Ockhi.

This plot clearly shows sea surface temperatures were more than 28.5^{0}C over the southwest Bay of Bengal (where the TC-Ockhi initially formed), which is much more than the SST threshold for formation of tropical cyclones. Over southeast Arabian sea, SSTs were even more than 29.0^{0}C. Many previous studies (for example, Jangir et al., 2021, Sanap et al., 2020) have documented the relationship between the ocean heat content and intensification of tropical cyclones. Fig. 4.19 shows the Tropical cyclone heat potential (TCHP), which clearly suggests the presence of large ocean heat content over southwest Bay of Bengal (Comorin area) and southeast Arabian sea (over the observed track of TC-Ockhi), TCHP was more than 70 KJ/cm^2. This large amount of heat potential was mainly responsible for the rapid intensification of TC-Ockhi.

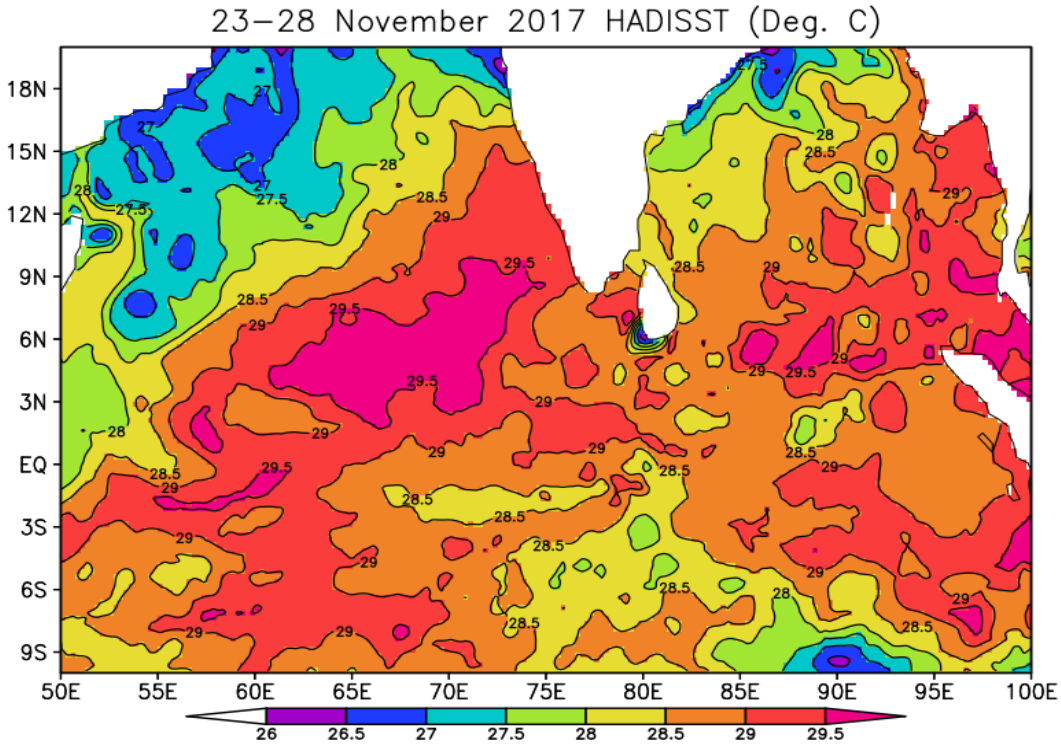

Fig. 4.18. Spatial distribution of Sea Surface Temperatures (SST) in ^{0}C averaged during 23-28 November 2017, just before the TC-OCKHI formed over southwest Bay of Bengal. Source: UK Met office, HADISST.

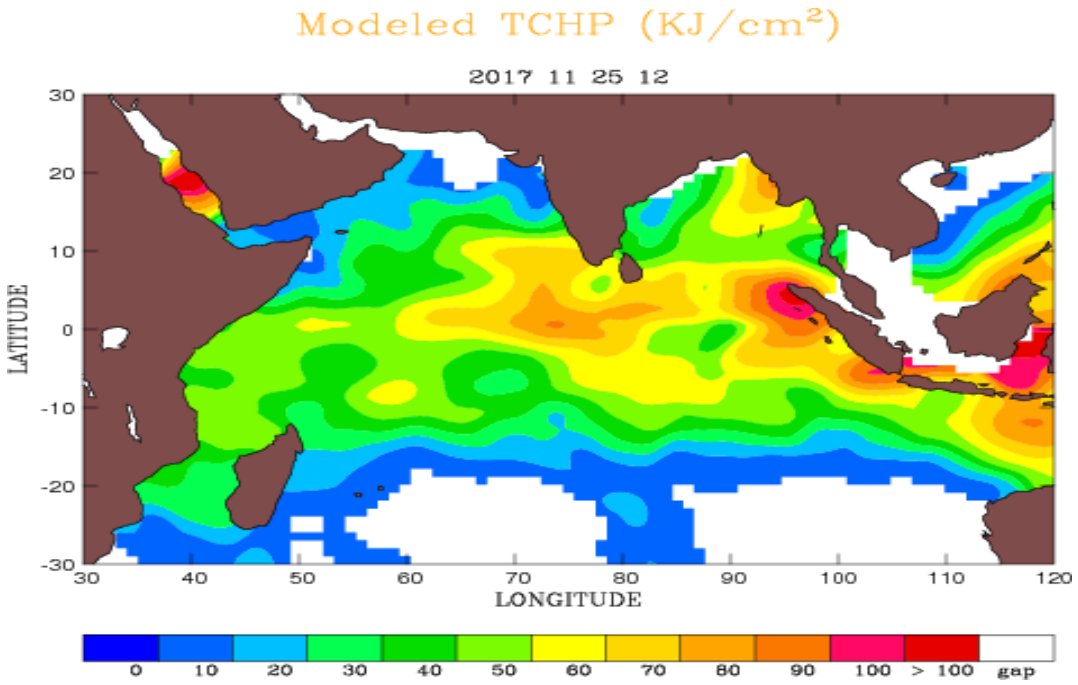

Fig. 4.19. Spatial distribution of Tropical Cyclone Heat Potential (TCHP) in KJ/Cm^2 on 25 November 2017, just prior to the formation of TC-OCKHI. Source: NRSC, ISRO.

Singh et al., (2020) studied the role of eastward moving Madden and Julian Oscillation (MJO) in the genesis of TC-Ockhi. Mohapatra and Adhikary (2011) also studied the role of MJO on tropical cyclone genesis over the Indian Ocean region. MJO is an eastward-moving wave in the tropical belt associated with enhanced convective activity in the regions from which it passes. Previous studies have shown that MJO in phase 4 is conducive for cyclogenesis in the south of Bay of Bengal by ensuing increased vorticity and anomalous cyclonic circulation on the westward side of MJO-induced convective activity. As the MJO propagated from phase 3 to phase 4 in November, 2017, it resulted in anomalous westerlies over the entire south Bay of Bengal (near the equator) in response to the shift in the convection over the maritime continent The anomalous westerlies along with anomalous easterlies over a narrow zone centred near 10°N, caused a strong shear zone and positive vorticity (Singh et al., 2020).

Jyothi et al., (2020) investigated the oceanic and atmospheric processes that have contributed to the Rapid Intensification (RI) and Rapid Weakening (RW) of Cyclone Ockhi using the HYbrid Coordinate Ocean Model (HYCOM) simulations and Global Forecast system (GFS) outputs. The environmental conditions prevailed before RI showed the presence of thick warm and fresh waters, ample supply of mid-tropospheric relative humidity, and moderate wind shear. The intrusion of dry air, strong vertical wind shear, and unfavourable oceanic conditions annihilated the storm intensity during the RW stage. Compared to the ocean temperatures, the vertical structure of salinity showed remarkable differences between the RI and RW locations resulting in contrasting upper-ocean stratification.

NWP Forecast Guidance for TC-Ockhi

India Meteorological Department (IMD) refers to many forecast products for preparing warnings for tropical cyclones over the north Indian Ocean. In this case of TC-Ockhi also, IMD had referred to many NWP products from IMD GFS, NCUM, ECMWF and JMA models. An analysis of inferences drawn from these models suggests that none of the models could provide an early forecast guidance for the genesis of TC-Ockhi as a Low/depression and its further intensification. The first model forecast guidance was available from the ECMWF model based on 28 Nov 0000 UTC in which the model indicated formation of a depression and its intensification into a severe cyclonic storm over the Arabian sea. The other models started indicating the formation of this system and its intensification from 29th Nov only. It is very important to note that none of the models correctly indicated the rapid intensification of TC-Ockhi during the course of its travel around the Comorin area.

However, the track forecasts by some of the models in predicting track of TC-Ockhi have been reasonably accurate as shown in Table-4.3 below. Numbers given in the bracket is number of verified forecasts. It can be seen that the Multi-Model Ensemble (MME) of IMD has the lowest errors compared to other models up to 48

hours lead time. Beyond 48 hours, ECMWF performed better than IMD-MME. The forecast errors of IMD-HWRF beyond 24 hours was far inferior compared to other models. The observed track of TC-Ockhi and IMD-MME predictions are given in Fig 4.20 and that of NCUM model are given in Fig 4.21. The models could indicate the recurvature and weakening of the TC-Ockhi very well.

In summary, the NWP models did not provide enough lead time for the IMD about its genesis over the Comorin area and its likely intensification into a cyclonic storm. IMD could get only 36 hours lead time to inform Kerala and Tamil Nadu government officials about its genesis and likely intensification. However, once the TC-Ockhi started moving, the forecast track errors were found reasonable and comparable with the climatological forecast errors. Despite considerable improvements in the prediction of genesis, intensity and track of cyclones in the north Indian Ocean in the recent decade, most of the models failed to capture the genesis of cyclone Ockhi in advance and its rapid intensification.

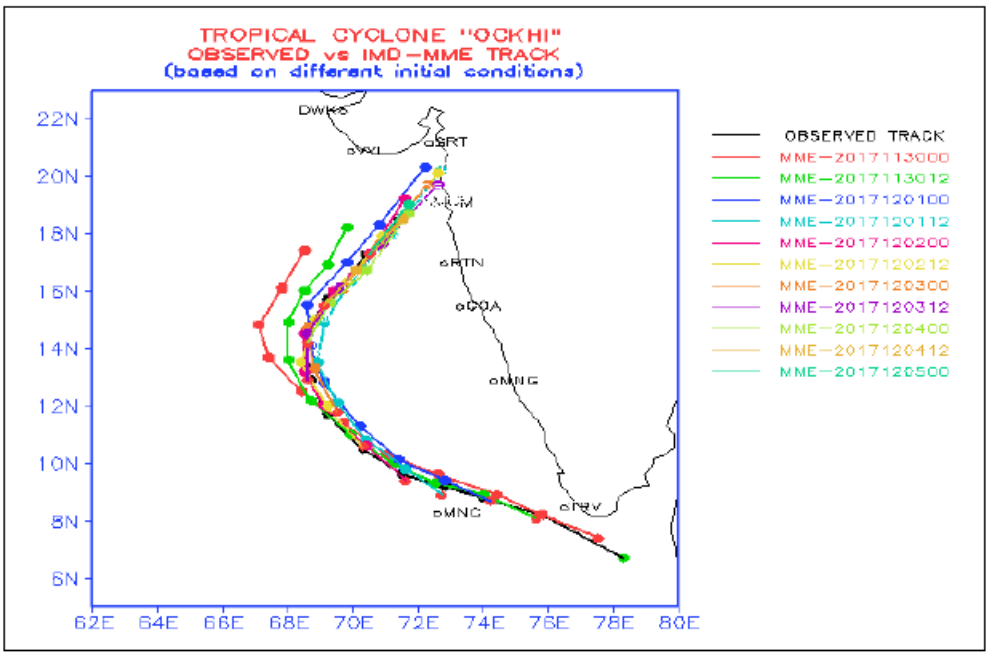

Fig. 4.20. Observed and Predicted track of TC-Ockhi by the IMD-MME prediction system.

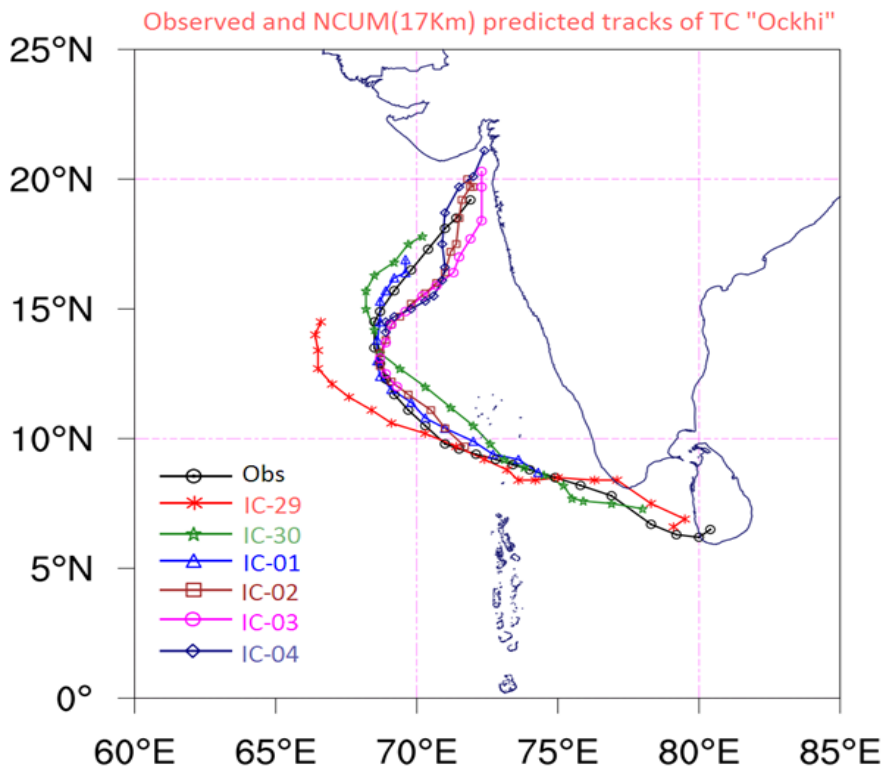

Fig. 4.21. Observed and Predicted track of TC-Ockhi by the NCUM prediction system.

A detailed study is required to understand why the NWP models could not provide adequate lead time in predicting the genesis and the further intensification of TC-Ockhi. One of the reasons could be that its genesis was very close to the equator. The models might have had problems in predicting its genesis near the equator. It may be mentioned that the models referred by IMD for forecast guidance are atmospheric models and do not treat the oceanic conditions and ocean-atmosphere coupling explicitly. This leads to an inference that even for short to medium range forecasting of weather systems like Tropical Cyclones, a coupled modelling strategy may be required.

This may be considered as a special case in which the NWP models had problems in predicting its genesis and rapid intensification. Otherwise, the recent NWP models are known for their accurate prediction of tropical cyclones.

Table 4.3

TC-OCKHI Average Track Forecast Errors in km by different models

(Source: IMD report)

Lead time	12 hrs	24 hrs	36 hrs	48 hrs	60 hrs	72 hrs
IMD-GFS	51(11)	68(10)	98(9)	117(8)	123(7)	145(6)
IMD-WRF	59(11)	115(10)	166(9)	226(8)	271(7)	278(6)
JMA	70(11)	70(10)	85(9)	103(8)	148(7)	215(6)
NCEP-GFS	60(11)	65(10)	75(9)	110(8)	91(7)	104(6)
UKMO	42(11)	63(10)	76(9)	122(8)	146(7)	173(6)
ECMWF	58(11)	69(10)	64(9)	62(8)	86(7)	100(6)
IMD-HWRF	58(21)	99(20)	130(18)	180(16)	234(14)	251(12)
IMD/MME	29(11)	44(10)	58(9)	86(8)	100(7)	112(6)
NCUM	82(13)	122(12)	129(11)	121(10)	144(9)	180(8)
NEPS	90(7)	134(6)	178(6)	217(5)	211(5)	208(4)

4.7. **Easterly Waves/Troughs in Easterlies**

From the Table 4.1, it is observed that easterly waves/trough in easterlies form a substantial portion of synoptic systems affecting south peninsula during the NE monsoon season. However, there are not adequate studies on easterly waves forming over the Indian Ocean.

Easterly wave is a wave within the broad easterly current and moves from east to west, generally more slowly than the current in which it is embedded. Although best described in terms of its wave like characteristics in the wind field, it also consists of a weak trough of low pressure. Easterly waves do not extend across the equatorial trough. To the west of the trough line in an easterly wave, there is generally found divergence, a shallow moist layer, and exceptionally fine weather. The moist layer rises rapidly near

the trough line; in and to the east of the trough line intense convergence, cloudiness and heavy rain showers prevail. Easterly waves occasionally intensify into tropical cyclones over the Bay of Bengal.

These waves are first identified in the Carribean (Dunn, 1940) and subsequently studied in detail over the African region using synoptic / satellite observations and numerical models. Considerable work on the passage of easterly waves over the African region, their structure, movement and roles in genesis of Atlantic hurricanes have been carried out and reports available in the literature (Burpee (1974), Jury et al., (1991), Berry and Thorncroft (2005) and Ross and Krishnamurti (2007)). Similar studies have also been undertaken for other oceanic regions such as Eastern and Western Pacific (Tai and Ogura, 1987). For the Indian region, Saha et al., (1981) have analysed 24 hour sea level pressure change charts of July-August of three stations for the 10 year period of 1969-1978 and have identified passage of westward propagating disturbances as predecessors to formation of monsoon lows and depressions. Using cross-correlation and power spectral analysis, they have determined the period of the wave as about 5 days, speed of about 6 ms^{-1} and wavelength of 2300 km. There are not adequate studies on Easterly waves forming over the Indian Ocean. Balachandran et al., (1998) have reported some features of an inverted V-type easterly wave over the Indian seas during December 1995 and have determined the speed of the wave as 8.2 knots using satellite imageries.

Conceptually, northerly meridional winds, subsidence, divergence and fair weather are the general atmospheric characteristics ahead of an approaching easterly wave trough and southerly meridional winds, rising motion, convergence and active weather are the characteristics behind the wave trough. The southerly meridional winds approaching the wave trough encounter an upgradient motion (moving from a low in the south towards a high in the north) and hence slow down leading to velocity convergence. The northerly winds approaching the wave ridge face a downgradient

motion as a result of which the wind speeds increase leading to velocity divergence. Thus, the winds approaching the wave trough are sub-geostrophic and the winds approaching the wave ridge are super-geostrophic (Hess, 1959). The pictorial representation of an easterly wave, taken from Riehl (1968, Tropical Meteorology) is given in Fig. 4.22.

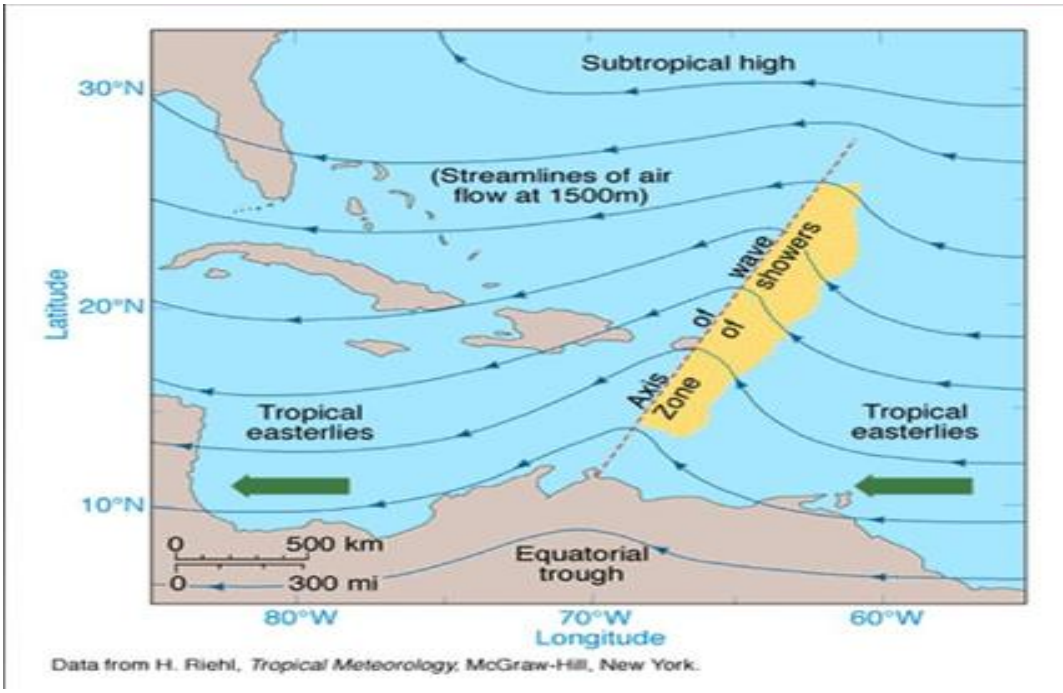

Fig. 4.22. Pictorial Representation of an Easterly Wave observed over the north Atlantic. After Riehl (Tropical Meteorology).

There are a few studies on examining the role of Easterly Waves for enhancing rainfall over south Peninsula during the NE Monsoon season. Reba et al. (2022) examined the years 2015, 2016 and 2017 to understand the variability of synoptic conditions including the propagation of easterly waves (EWs). Further, it is also seen that many active rainfall spells during 2015 and 2017 over Tamil Nadu met-subdivision were associated with passage of EWs over the southern peninsula along east of 85^0E, whereas, the large deficient NE monsoon of 2016 witnessed no such active spell of

monsoon and the passage of EW was confined to the eastern part of Bay of Bengal and never entered into the Indian peninsula. Geetha and Balachandran (2014) studied the easterly wave characteristics during 2010 NE monsoon season by means of synergetic analysis using synoptic, statistical and numerical methods. The easterly waves during 2010 had time periods of about 4.5 days. The speed of movement, wavelength and amplitude of EWs were 7.28 ms^{-1}, 2800 m, and 6.7 ms^{-1} respectively. Sanap et al. (2018) examined the 2015 NE Monsoon season in respect of easterly wave activities. Their results indicated that EW activity over the Indian Ocean plays a seminal role in occurrence of heavy rainfall events during the positive phase of the ENSO (El-Niño), while it is found to be weak during negative (La-Niña) and neutral phase.

Here, we now discuss on a case study of formation of an easterly wave and its westward movement across south peninsula during 13-18 November, 2010. As shown in Fig. 4.23, there was widespread rainfall activity over south peninsula and adjoining Bay of Bengal associated with the Easterly wave. It is interesting to note that a wave type structure is observed in precipitation pattern during this period. Fig. 4.24 shows the vector winds at 700 hPa during the period 13-18 November, 2010 and vorticity at 700 hPa. Positive vorticity suggesting large scale ascending motion can be noticed on the eastern side of the trough line of the easterly wave. The easterly wave which formed over southeast Bay of Bengal moved westwards and crossed south peninsula by 17 November and emerged into the Arabian sea on 18th November. This weather system caused widespread rainfall activity over the region. The relevant satellite pictures of this easterly wave are shown in Fig. 4.25.

Fig. 4.26 shows the Longitude-Time cross section of a) Meridional wind at 700 hPa b) Outgoing Longwave radiation c) Precipitable water content and d) Precipitation rate at 10^0N during the period 13-18 November 2010, showing different aspects of an easterly wave, which travelled from east to west during 10-20 November, 2010 and contributed to large scale rainfall activity over south peninsula. These plots

very clearly show the westward movement of easterly wave representing meridional winds at 700 hPa, OLR, precipitation rate and vertical velocity, omega. The zero-line separating southerlies and northerlies is shown in Fig. 4.26. It is interesting to note that lower values of OLR, large precipitation rate and large ascending motion (negative omega) are observed east of the zero line. This suggests that in and to the east of the trough line intense convergence, cloudiness and heavy rain showers prevail.

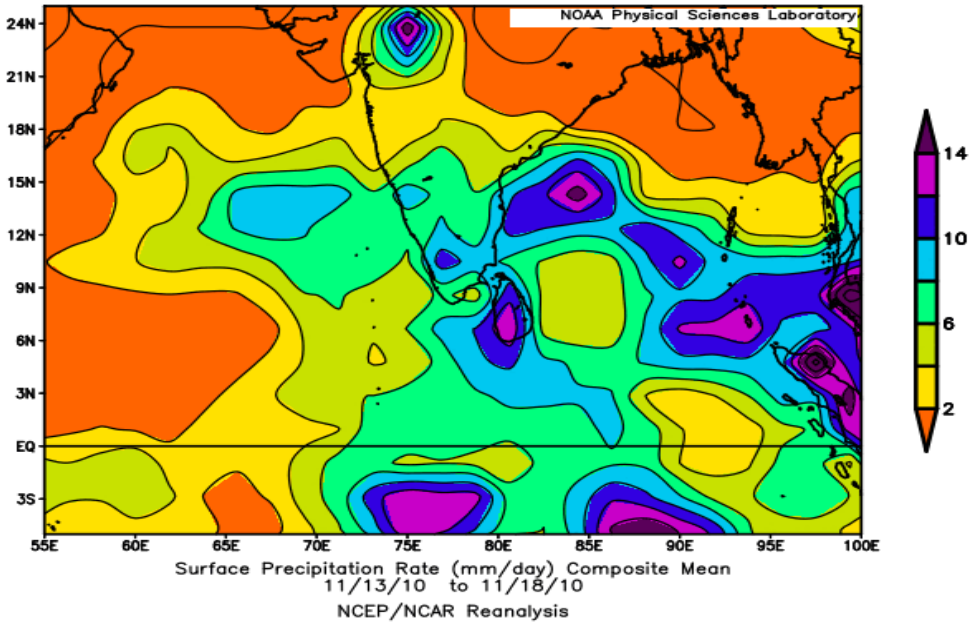

Fig. 4.23. Precipitation rate (mm/day) averaged during 13-18 November 2010 associated with the Easterly Wave. Source: NCEP/NCAR reanalysis.

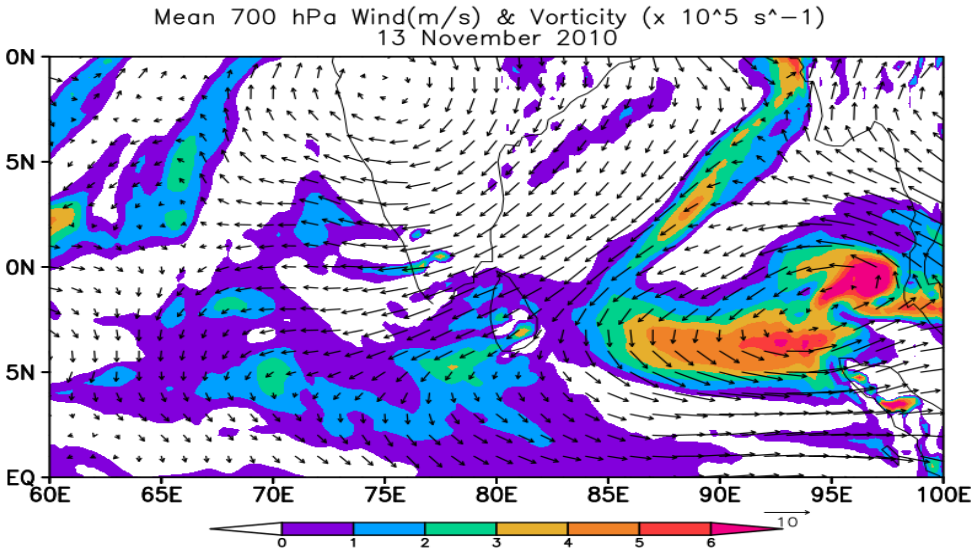

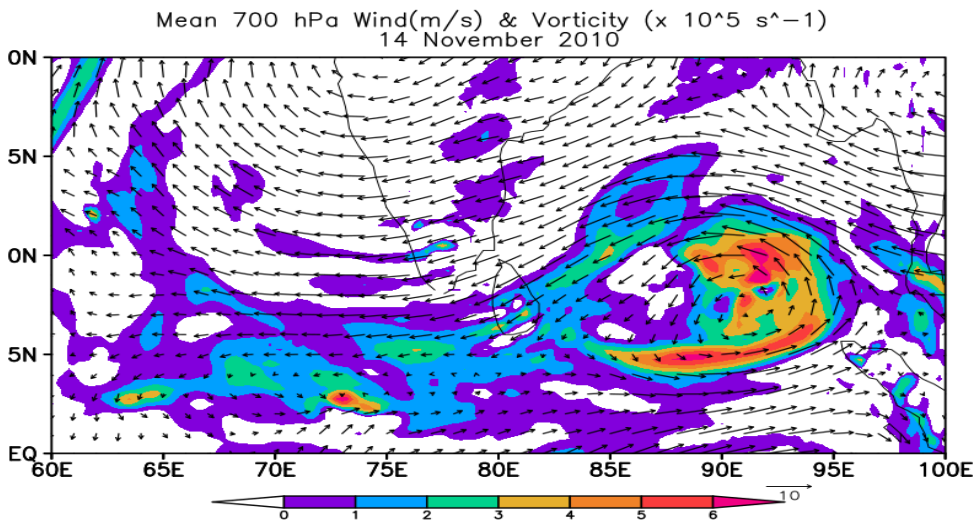
Mean 700 hPa Wind(m/s) & Vorticity (x 10^5 s^−1)
14 November 2010
0N
5N
0N
5N
EQ
60E
65E
70E
75E
80E
85E
90E
95E
100E
10
0
1
2
3
4
5
6

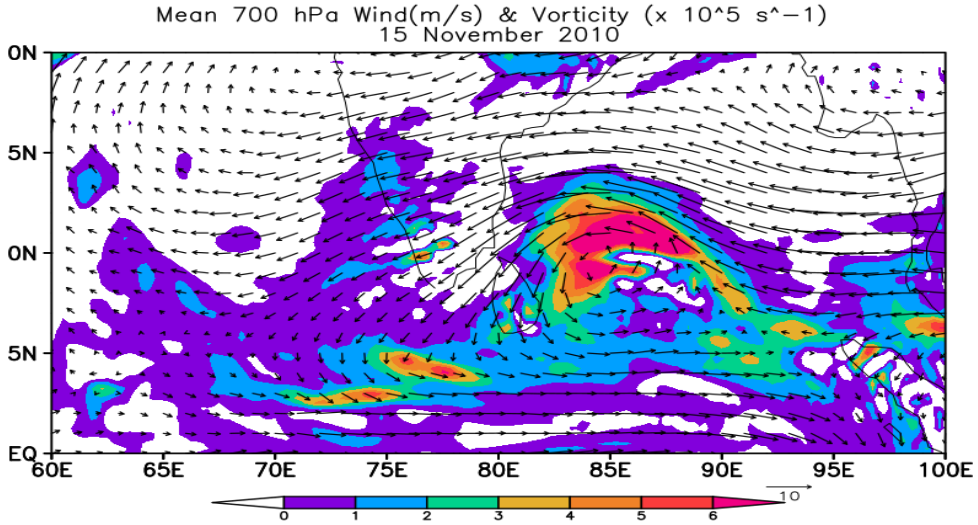
Mean 700 hPa Wind(m/s) & Vorticity (x 10^5 s^−1)
15 November 2010
0N
5N
0N
5N
EQ
60E
65E
70E
75E
80E
85E
90E
95E
100E
10
0
1
2
3
4
5
6

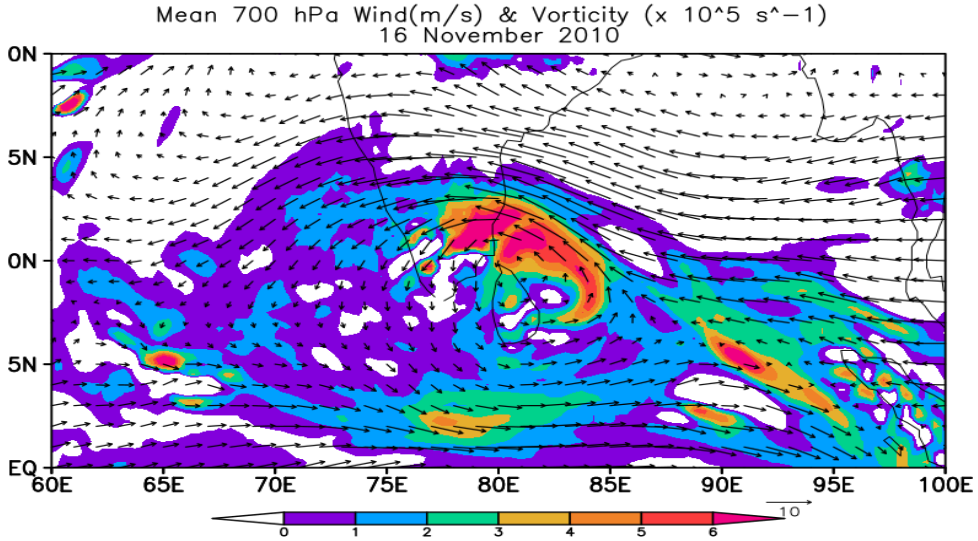
Mean 700 hPa Wind(m/s) & Vorticity (x 10^5 s^−1)
16 November 2010
0N
5N
0N
5N
EQ
60E
65E
70E
75E
80E
85E
90E
95E
100E
10
0
1
2
3
4
5
6

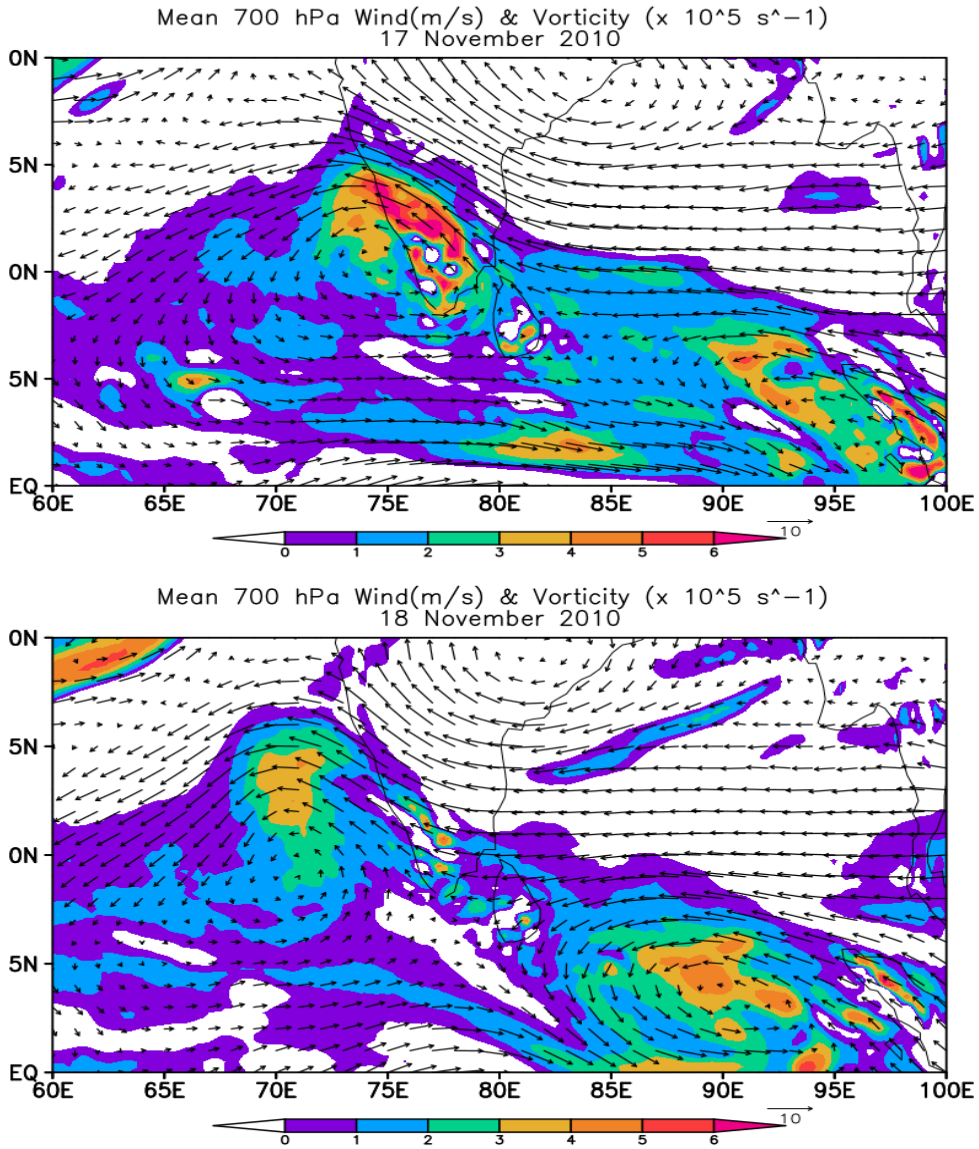

Fig. 4.24. Spatial distribution of 700 hPa winds and vorticity from 13 -18 November, 2010, showing westward movement of an easterly wave, which caused widespread rainfall activity over south Peninsula.

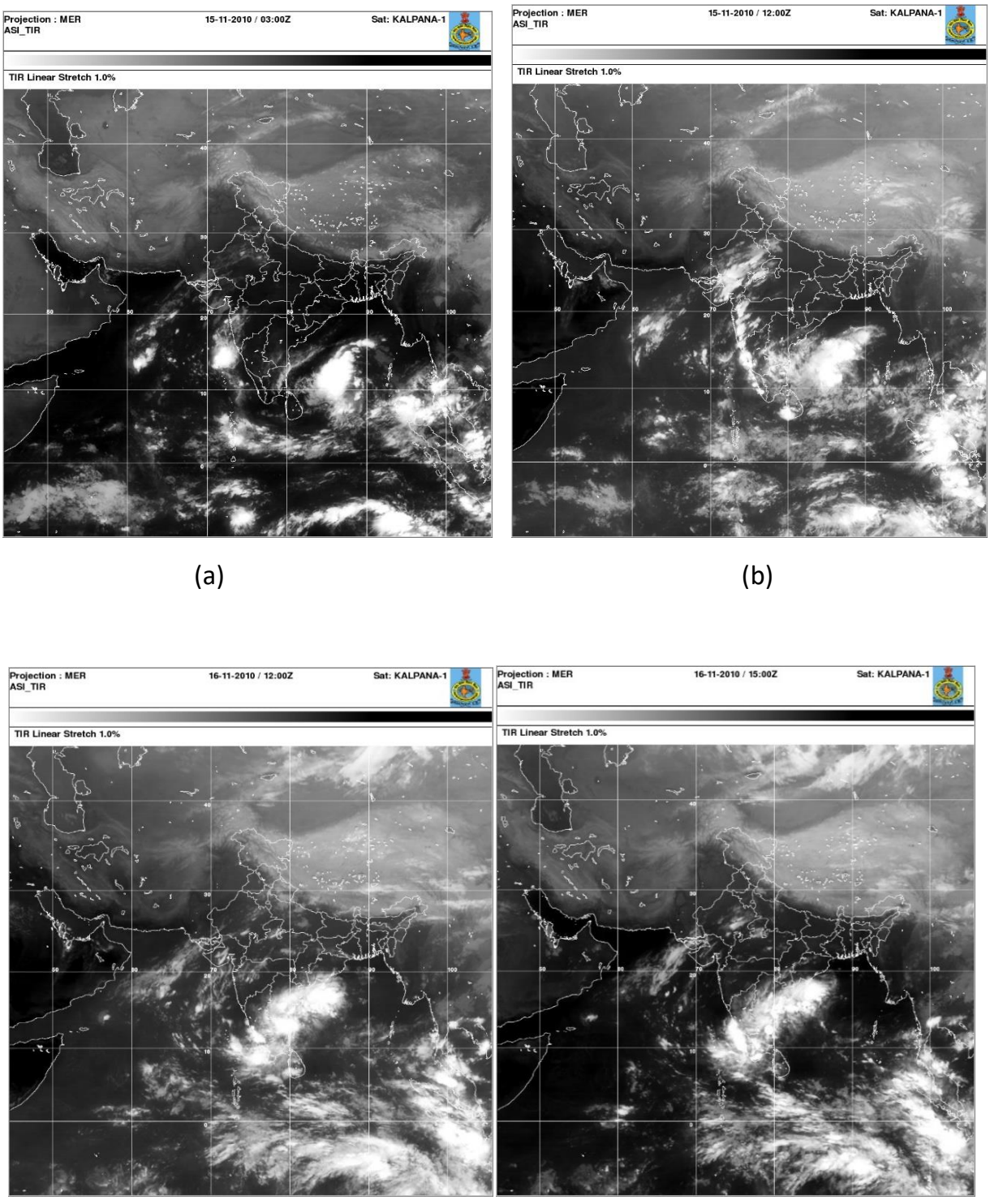

Fig. 4.25. Kalpana IR Satellite Pictures showing the presence of easterly wave over the Bay of Bengal. a) 0300 UTC 15 November b) 1200 UTC 15 November, C) 1200 UTC 16 November and d) 1500 UTC 16 November. Source: IMD Satellite Directorate.

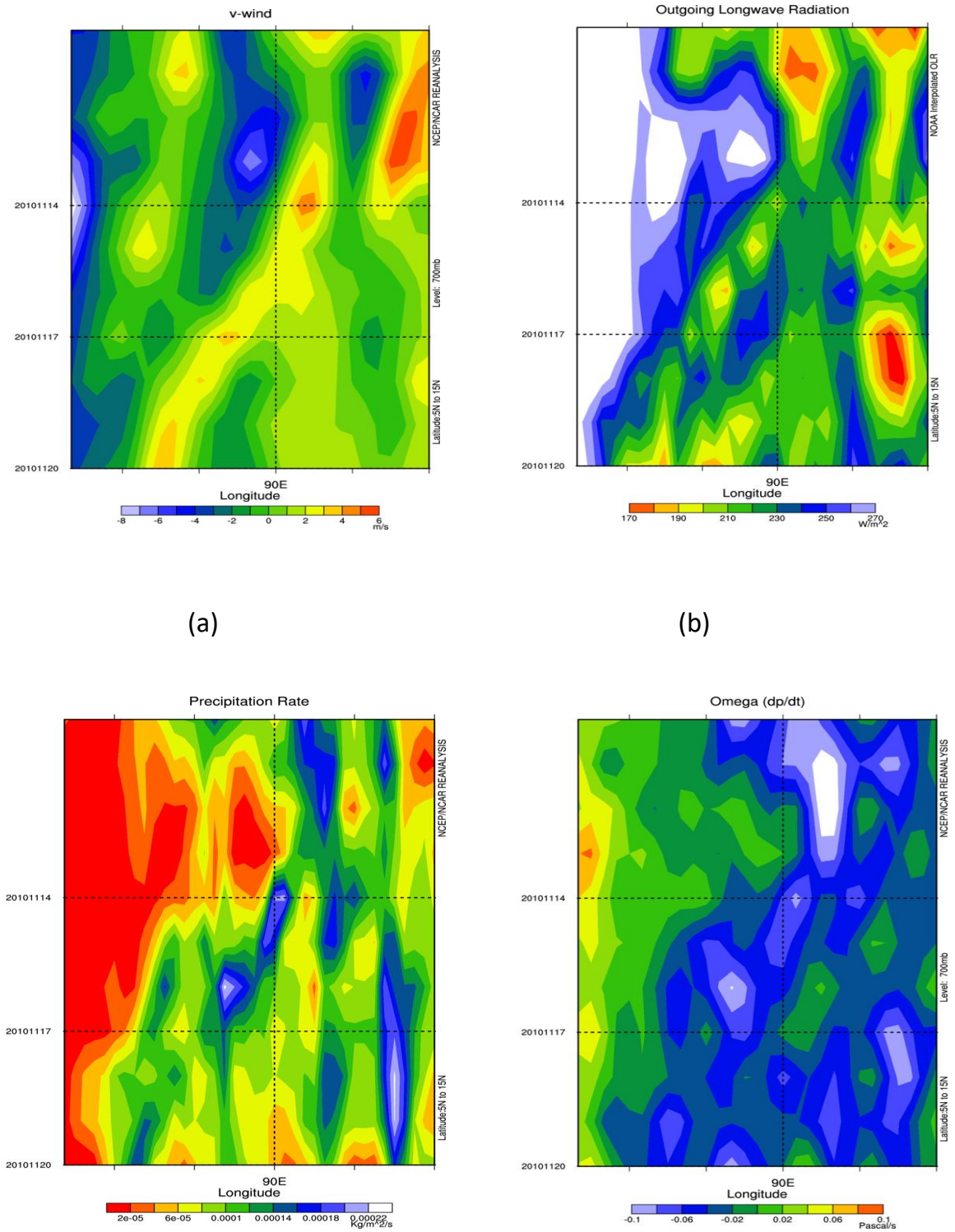

Fig. 4.26. Longitude-Time cross section of a) Meridional wind at 700 hPa b) Outgoing Longwave Radiation (OLR) c) precipitation rate and d) vertical velocity, Omega averaged between 5-15^{0}N during the period 10-20 November 2010